2011

# Novel Thermal Analytical Techniques to Characterize Drugs and Drug Delivery

Lakshmi Swetha Kaza
*Cleveland State University*

# NOVEL THERMAL ANALYTICAL TECHNIQUES TO CHARACTERIZE DRUGS AND DRUG DELIVERY

**LAKSHMI SWETHA KAZA**

Bachelor of Science in Pharmacy

ANDHRA UNIVERSITY

May, 2008

Submitted in partial fulfillment of requirements for the degree

**MASTER OF SCIENCE IN CHEMISTRY**

at the

**CLEVELAND STATE UNIVERSITY**

August, 2011

This thesis has been approved

for the Department of CHEMISTRY

and the College of Graduate Studies by

_____

"Thesis Chairperson", Dr. Bin Su

_____

Co-chair, Dr. Alan.T Riga

_____

Dr. Stan Duraj

_____

Dr. Robert Wei

Date: July 26, 2011

## ACKNOWLEDGEMENTS

Foremost, I would like to express my deep and sincere gratitude to my advisor Dr. Alan Riga for the continuous support for my Master's thesis research, for his patience, motivation, enthusiasm, and immense knowledge. His guidance helped me in all the time of research and writing of this thesis. His wide knowledge and his logical way of thinking lead me working on diverse exciting projects. His understanding, encouraging and personal guidance have provided a good basis for the present thesis. Besides my advisor, I would like to thank the rest of my thesis committee members, Dr. Bin Su, Dr. Stan Duraj, and Dr. Tobili Sam Yellowe for their encouragement and insightful comments. I am indebted to all of my colleagues, Dr. Indika Perera, M. Ellen Matthews, Shravan Thakur, Manik Pavan Maheswaram, Hareesha Venumuddala and Dhruthiman Mantheni for their support in writing the thesis and stimulating discussions. Last but not the least; I would like to thank my parents and my sister for supporting me spiritually throughout my life. Without their financial support and understanding it would have been impossible for me to finish this work. I want to thank Dr. Sun, Nandana and V. Prathima for helping me to use UV- Spectroscopy equipment.

**NOVEL THERMAL ANALYTICAL TECHNIQUES TO CHARACTERIZE DRUGS AND DRUG DELIVERY**

LAKSHMI SWETHA KAZA

## ABSTRACT

This thesis encompasses three significant projects. The study includes the characterization and evaluation of the properties of a commercial contraceptive transdermal patch, Ortho Evra® by Dielectric Analysis and Differential Scanning Calorimetry (DSC). This study helps in monitoring the mobility of the drug and transport properties by Isothermal and Scanning Dielectric Analysis as a function of temperature and frequency**.** The drugs in this product are norelgestromin and ethinyl estradiol. DSC was used to detect any crystalline character of the drugs by their fusion properties. Having no melting endotherm and detecting a glass transition temperature suggested that the drugs in the patches were amorphous. The amorphous form of the drug has more bioavailability. The isothermal DEA a plot of Log frequency vs. reciprocal temperature (K) revealed two critical modulating frequencies at body temperature 37°C for the two API drugs with DEA peak frequencies at 460 and 560 Hz.

The main project includes studying the polarization of macro and micro molecular liquid drugs by Dielectric Analysis, B-Cell (a customized isothermal dielectric device) and Differential Scanning Calorimetry. This study demonstrated *in vitro* transport of selected non-ionic high (e.g. insulin) and low (e.g. Diphenhydramine) molecular weight drugs through excised biological tissue membranes using alternating current (AC) electrokinetics. This new technique of the drug delivery system enhances benefits over systemic oral therapies, in which clinically sufficient quantities of the active ingredient

do not reach the intended target organ and/or use of the drugs result in serious side effects. An optimally-tuned low-voltage applied AC electrical field has been found capable of inducing polarization and delivering micro and macromolecules through a biological membrane. The relationships between factors such as delivery time, AC voltage amplitude and frequency, and transported drug concentration were investigated. A factorial design was used to establish experimental parameters for the insulin solution evaluating DEA variables of voltage, frequency, time, temperature, drug dose, and membrane thickness. A clear result of the experimental design for insulin was that the low frequency was significant in enhanced drug delivery. Dielectric Analysis was used to modulate the drugs delivery response measured by a change in the log conductivity vs. log frequency curve at a lower frequency of 500 Hz and a higher frequency of 1000 Hz for insulin at 37ºC. Imposition of a low frequency of 500 Hz aliened dipoles and higher frequency aided the mobility of the drug ions into the biomembranes. The delivery was confirmed qualitatively and quantitatively by enhanced conductivity for the drugs based on the "polaron theory" of conductivity or the "hopping model" and UV spectroscopy.

The third project includes a study to develop a standard protocol to determine the water content and type by thermal analysis of Milk of Magnesia. Differential Scanning Calorimetry (DSC) and Thermal Gravimetric Analysis (TGA) were used in a novel manner for examining the commercial pharmaceutical suspensions and to note the difference between the brand and the generic forms.

## TABLE OF CONTENTS

**PAGE**

## LIST OF FIGURES

**PAGE**

CHAPTER V



CHAPTER VI

## LIST OF TABLES

**PAGE**

CHAPTER VI

## ABBREVIATIONS

DEA- Dielectric Analysis

DC- Direct Current

AC- Alternative Current

DSC- Differential Scanning Calorimetry

SFI- Solid fat index

$\Delta H_f$- Heat of Fusion

$T_m$ - Melting Temperature, extrapolated endothermic onset temperature

$T_p$- Peak Melting endothermic Temperature

$\Delta H_c$-Heat of exothermic Crystallization

$T_c$- Crystallization Temperature, extrapolated exothermic onset temperature

$T_{cp}$- Peak exothermic Crystallization temperature

$\Delta H_v$ - Heat of endothermic Vaporization

$T_v$ - Vaporization temperature, extrapolated endothermic onset temperature

$T_{vp}$ - Peak Vaporization temperature

$T_g$ -Glass transition temperature

UV-vis- Ultraviolet-visible spectroscopy

Mom- Milk of Magnesia

TG- Thermogravimetry

ASTM- American Standards for Testing Materials

ECA- Electrical Conductivity Analysis

## OBJECTIVES

The main objective of this thesis was to study the polarization of macro and micro molecular liquid drugs by Dielectric Analysis, a customized B-Cell and Differential Scanning Calorimetry. Evaluation of a commercial contraceptive transdermal patch, Ortho Evra® using DEA aided in monitoring the mobility and transport properties of the two drugs transdermally. DSC supplied information on the amorphous content of the drugs, the low density polyethylene backing substrate that melted at 106$^{o}$C, and the Tg at -20$^{o}$C of the adhesive suggests styrene butadiene rubber (SBR) latex in a low molecular weight resin.

The delivery of the drug was confirmed quantitatively by recording the enhanced conductivity of the drug in the bio-membrane and the drug throughput by calibrated UV analysis. DEA was used to modulate the drugs delivery response measured by a change in the log conductivity vs. log frequency curve at a low and a higher frequency. The consequence of this Ortho Evra research helps in developing an AC electrified transdermal patch for Diabetic patients in which there is a controlled release of insulin to be associated with a consumer's blood glucose level.

Thermal Analysis aided in the development of a protocol to distinguish the water content in the brand and generic forms of commercially available Milk of Magnesia suspension and by difference in the total mass minus the water content revealed the magnesium hydroxide content.

## HYPOTHESIS

The transdermal route provides continuous mode of administration of the drug especially for protein and peptides having short half-lives. Skin is low in proteolytic activity thus minimizing the degradation of the drug at the site of administration. Transdermal patches are available in market for various drugs, but are limited to small lipophilic molecules which can passively diffuse through the skin. Hydrophilic and macromolecular drugs have low skin permeability in which electrical forces aids in drug transport across the skin. Iontophoresis which uses Direct current (DC) is the most commonly used electrical forces for transdermal patches. A number of adverse effects are reported as a result of high applied voltages causing skin irritation and erythema. However, this approach results in uncomfortably long treatment times. Iontophoresis replaced by AC electric field would be a novel method for the drug delivery minimizing the adverse effects. It is important to have a sensitive method to characterize the transport properties of the drugs by AC electric field. The commercial DEA instrument and the customized B-cell yielded electrical properties of the drugs and their behavior and performance in the drug delivery**.** Throughput in our study is based on an evaluation of a closed system and measuring the drug content by UV Analysis. The DEA conductivity of the aqueous solution drug at the end of test should be related to the efficacy of the drug delivery. Basic transdermal patch material and transport properties can be determined. Evaluation of a commercial patch will discover the fundamental properties needed for the patch development.

## PROTOCOL

Characterization and Transport Properties by Thermal– Bio-analytical Techniques

*Synopsis*

- Characterization of commercial contraceptive transdermal patch, Orthoevera™
- Study the transport properties and polarization of macro and micro molecular drugs.

*Terminology*

- All the significant terms are well defined
- Defined all abbreviations

*Scope*

- Qualitative and Quantitative measurements (DEA and UV)
- Physical and electrical properties of the drugs are evaluated

*Hazards*

- Care should be taken in handling specific drugs

*Methods*

- Dielectric Analysis
- Ultraviolet –Visible spectrometry
- Differential Scanning Calorimetry
- Thermalgravimetry
- Lab wave 9000 Moisture Analyzer
- Oven dry method

*Summary of Methods*

- Instruments used in this study are briefly described

- Test method principle

*Calibration*

- Detailed instructions of calibration of the instrument are cited

*Significance in Use*

- New approach for the Development of Transdermal Patches
- Study of the Drug properties

*Procedure*

- Standard protocols were performed for calibration of instruments
- Describe successive steps for all the procedures

*Interpretation of results*

- Directions for evaluating the results
- List of all the tables
- Specify significant figures

*Research report*

- Detailed information required in reporting the results
- Correlating the results

*References*

- References to publications providing needed information
- Keywords: Identify words, terms or phrases that best represent the technical information reported

*Conclusions*

- Summarize all collected data
- Compare data from different methods

# CHAPTER I

## INTRODUCTION

Transdermal drug delivery has made significant contribution to medical field, standing as a better alternative to oral drugs and to the use of hypodermic injections too. The use of topical medications to treat local infections on skin was in practice from many years but the use of transdermal delivery system was becoming a well known practice from a few decades. The scopolamine patch to treat motion sickness was first of its kind to be formulated as a transdermal drug. Later the use of nicotine patches has become popular to aid smoking cessation. Currently there are about 19 different transdermal delivery systems available for hormones such as estradiol and testosterone and analgesics such as fentanyl. Combination patches are available for contraception and hormone replacement therapy.[1] Some of the most commonly used transdermal patches are as follows: nicotine patch which releases nicotine for about 16 hours and prevent the carving of cigarette by smokers, scopolamine patch which shows the effect for about 3 days, used to treat motion sickness and also in post operational nausea, fentanyl patch which has its pain relieving effect for about 72 hrs and estrogen-progestin contraceptive

need to be taken only once a week rather than taking a pill every day.[2] This extended release formulation provides better patient compliance.

*Advantages*

Transdermal systems are non-invasive and can be self-administered. Controlled release of the medication is one of the advantages over other formulations like oral and topical. It prevents gastrointestinal irritation which is more common effect seen with oral formulations. This route of drug delivery bypasses the first pass effect of the liver which is a potential advantage over oral formulation of drugs. It avoids multiple dosing of drugs thus enhances patient compliance. They also improve patient compliance and the systems are generally inexpensive.

*Barrier*

But one of the major drawbacks of this system is that skin being an effective barrier; it is restricted only to the delivery of certain low molecular weight, lipophilic drugs. The exploitation of transdermal drug delivery for the delivery of hydrophilic drugs, peptides and macromolecules always remained as one of the great challenges. Skin is composed of outer thick layer, stratum corneum which is about 10-20 µM thick. Below this layer is epidermis which lacks blood vessels and measures about 50-100 µM. The underlying layer beneath the epidermis is dermis which has blood capillaries suitable for drug absorption. The major hindrance for the drug particles is stratum corneum, composed of corneocyte cells cross-linked with keratin and intracellular spaces are filled with a mixture of lipids arranged in bi-layers. Transport of drug particles through this complex structure is a great ordeal that is faced. This necessitates the use of enhancers

that facilitate the transport of drug molecules by enhancing permeability of stratum corneum.

*Stages of transdermal drug development*

The first generation transdermal drug delivery involved the delivery of lipophilic and small molecules using traditional patch system. A typical scopolamine patch has an outer backing layer which is impermeable, underneath of which a drug reservoir is present. [1] Then a rate limiting membrane is present which controls the rate of drug delivery from the reservoir, followed by an adhesive layer that sticks to the skin. A protective layer is present which is removed just before using the patch. This generation has been successful in delivering certain drugs.

The second generation advanced a little bit by using conventional chemical enhancers to deliver other hydrophilic molecules. The enhancers used include Azone (1-dodecylazacycloheptan-2-one) and SEPA (2-n-nonyl-1,3dioxolane).[2] But the use of chemical enhancers is not very much successful in delivering hydrophilic and macro molecules because these chemicals disrupted the inner skin layers. Other techniques like iontophoresis and non-cavitational ultrasound have also been used. Iontophoresis increase transdermal drug delivery by typically applying a continuous low-voltage current. Iontophoresis does not affect the skin permeability but enhances drug transport by providing an electrical driving force which makes it as an adjuvant method. [3,4] Because Iontophoresis does not primarily change the skin barrier itself, it is mostly applicable to small molecules that carry a charge and some macromolecules up to a few

thousand Daltons, so this technique could not be an ideal technique for the delivery of macromolecules and vaccines.

The third generation made use of cavitational ultrasound, Micro needles and electroporation methods which are based on the principle of disrupting stratum corneum on a nanometer scale. [5] Ultrasound generates cavitation, which is the formation, oscillation and, in some cases, collapse of bubbles in an ultrasonic pressure field.[6] This cavitation bubbles concentrate the energy of ultrasound and thereby enable targeted effects at the site of bubble activity for the transdermal drug delivery.[7] Although effective, applications of cavitational ultrasound may be limited by the need for a sophisticated device that only increases skin permeability at the nanometer scale and thereby may not be broadly applicable to macromolecules and vaccines. Electroporation uses short, high-voltage pulses, a method to reversibly disrupt cell membranes for gene transfection and other applications. It has shown to disrupt lipid bi-layer structures in the skin.[8] During electroporation the electric field applied for milliseconds provides an electrophoretic driving force. Diffusion through long-lived electropores can persist for up to hours, such that transdermal transport can be increased by orders of magnitude for small model drugs, peptides, vaccines and DNA [9]. Recently, electroporation was shown to deliver a model peptide vaccine into the skin of mice to generate a strong cytotoxic T lymphocyte response.[10] Although electroporation has been studied extensively in animals, this approach to transdermal delivery has received limited attention in humans because of the complexity of device design.

Limitation of diffusing large compounds through micron-scale disruptions, a long time to diffuse through, longer treatment times, a very small amount of transported

molecules, and therapeutically insufficient amount of drug passing through in the majority of applications leads us to develop novel thermal analytical techniques to characterize drugs and drug delivery. The main goal of this study is to investigate various variables and optimize the conditions such as length of treatment and low currents for effective transdermal drug delivery of macromolecule e.g. insulin.

## References


1. Morgan TM, Reed BL, Finnin BC. Enhanced skin permeation of sex hormones with novel topical spray vehicles. *J Pharm Sci.* 1998;87:1213–1218
2. Williams AC, Barry BW. Penetration enhancers. *Adv Drug Deliv Rev.* 2004; 56:603–618.
3. Banga AK. London: Taylor & Francis; 1998. Electrically-Assisted Transdermal and Topical Drug Delivery.
4. *19.* Kalia YN, Naik A, Garrison J, Guy RH. Iontophoretic drug delivery. *Adv Drug Deliv Rev.*2004;56:619–658.
5. Arora A, Prausnitz MR, Mitragotri S. Micro-scale devices for transdermal drug delivery. *Int J Pharm.*2008
6. Wu J, Nyborg W, editors. London: Imperial College Press; 2006. Emerging Therapeutic Ultrasound.
7. Ogura M, Paliwal S, Mitragotri S. Low-frequency sonophoresis: Current status and future prospects. *Adv Drug Deliv Rev.* 2008
8. Denet AR, Vanbever R, Preat V. Skin electroporation for transdermal and topical delivery. *Adv Drug Deliv Rev.* 2004;56:659–674.
9. Li S, editor. Totowa, NJ: Humana Press; 2008. Electroporation Protocols: Preclinical and Clinical Gene Medicine.
10. Zhao YL, et al. Induction of cytotoxic T-lymphocytes by electroporation-enhanced needle-free skin immunization. *Vaccine.* 2006;24:1282–1290

# CHAPTER II

# INSTRUMENTATION

## 2.1. Dielectric Analysis

Dielectric Analysis (DEA) is a thermo analytical technique used to measure changes in electrical properties of a sample, liquid or solid, as a function of temperature, time, and frequency. The two fundamental electrical characteristics that DEA can measure for a sample are *Capacitanc*e (High frequency permittivity (e') or dielectric constant) and *Electrical conductivity (pS cm$^{-1}$)* (Loss factor (e") * applied frequency (Hz) * a constant). DEA measures three main parameters over a wide range of frequencies (e.g. 0.10 to 300,000 Hz): the *loss factor (e")* which is related to the energy required to align dipoles and move ions and is converted into the ionic conductivity (pS/cm*).* The *permittivity (e')* is another physical property and is related to the dipole content. *Tan Delta* is a ratio of loss factor divided by the permittivity, (e"/e'). An applied sinusoidal voltage on a sample placed on a sensor creates an alternating electric field, inducing polarization of the sample and followed by facilitate transport of the polarized drug through a bio-membrane.

***Figure 1:*** *TAI Dielectric Analyzer 2970*

Isothermal DEA procedure determines the polarization time of a sample and helps in better understanding of the chemistry and molecular mobility that relates to the structure of the drug. DEA is ultra-sensitive, and can measure conductivity from $10^{-3}$ $pScm^{-1}$ and as high as $10^{12}$ $pScm^{-1}$. DEA measures changes in dipole orientation and ion mobility of the sample.

*2.1.1. Instrument*

Dielectric Analyzer (DEA) TA instrument (TAI) 2970 was used in this study. Parameters such as temperature, sampling size, sample placement, calibration of the sensor and temperature, are to be taken into consideration. The DEA can test various forms of samples, i.e. gels, solutions, solids, powders, and thin films. Four types of sensors exist for the TA Instruments DEA: parallel plate, single surface, sputter coated and remote single surface. [2] Single surface gold ceramic inter-digitated electrodes are used for the experiments. Measurements can be taken within a temperature range of -100

ºC to 300 ºC and through a frequency range of 0.1 - 300k Hz. Dry nitrogen gas or air gas purge at a flow rate of 50 $mLmin^{-1}$ is used.

### *2.1.2. Calibration*

New test procedures were applied that describes the temperature calibration of Dielectric Analyzers with pharmaceuticals over the temperature range from 25°C to 250°C. This procedure uses pure Active Pharmacy Ingredients (APIs). This test method can be used with a universal standard protocol for DEA. This new standard test method can employ devices from a variety of commercial companies. Calibration is performed by observing the melting transition temperature of standard Pharmaceutical materials within the temperature range of interest.

Pharmaceutical test specimens (calibrants) of established melting temperatures are evaluated in a closed system typically in a nitrogen atmosphere over a specific temperature range. The test calibrants are evaluated by DEA using an interdigitated electrode array (IDA) over a specific temperature range. At the transition temperature of the test specimen, there is a change in permittivity which is recorded. These melt transition temperatures of test specimens obtained from DEA data are compared directly to the known literature melt transition temperatures.

The calibration materials used in this test development are: Acetanilide (Tmp, 113-116°C) and Acetophenetidin (Tmp, 132-138°C).[7,8] These test protocols were accomplished based on the Standard Test Method for temperature calibration of DEA and ASTM E 2038 [1]. The preliminary $R^2$ coefficient of correlation for known literature transition temperature vs DEA Permittivity melt temperature for the calibrants was 0.98.

These new pharmaceutical based test protocols, permit inter-laboratory comparison and intralaboratory correlation of instrumental temperature scale data within the pharmaceutical community, and will be implemented in our chemical pharmaceutical research.

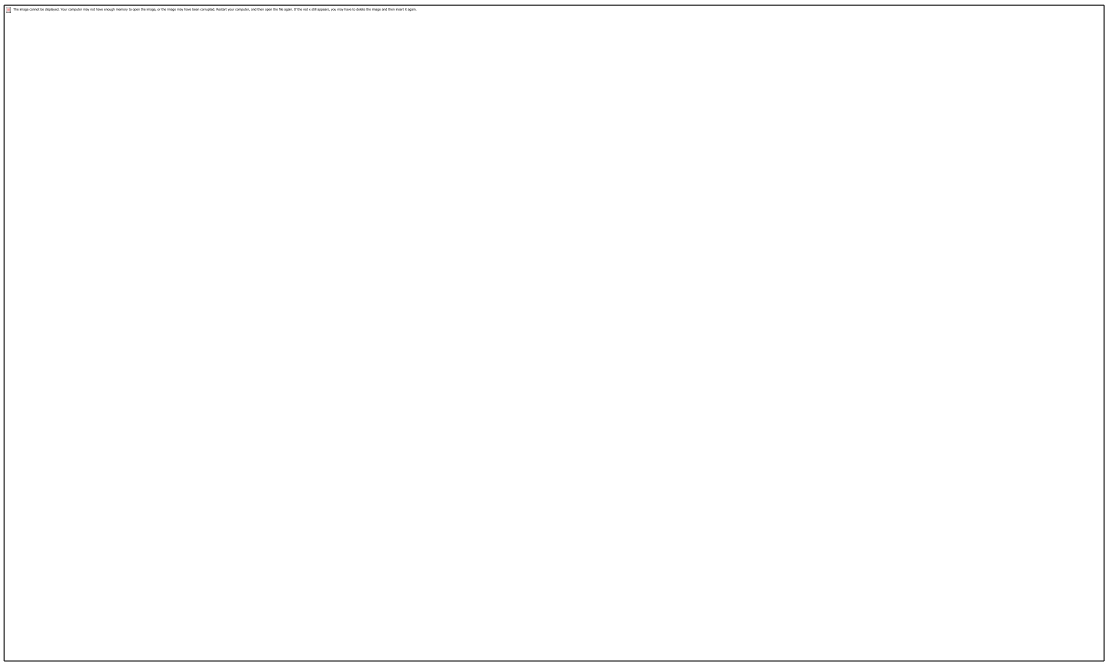

***Figure 2:*** *DEA curve of Acetanilide showing Log permittivity and Derivative of Log permittivity transition temperature at 1 Hz frequency.*

A summary of frequency used i.e. (single or set of 4 frequencies); permittivity and Log permittivity transition temperature obtained from the DEA thermal curves of the calibration materials are listed in: Acetanilide, table 1;

| Frequency (Hz) | Permittivity Transition Temperature °C | Log Permittivity Transition Temperature °C |
|---|---|---|
| **1000 Hz** | 114 | 113 |
| | | |
| **1Hz** | 116 | 113 |
| **10 Hz** | 115 | 113 |
| **100 Hz** | 114 | 114 |
| **1000 Hz** | 114 | 114 |
| | | |
| **Average** | 115 | 113 |
| **Std Deviation** | 0.89 | 0.55 |
| **% Relative Error** | 0.77 | 0.48 |

***Table 1****: Acetanilide Tmp (113-116) °C; DEA Permittivity and Log Permittivity Transition Temperature of single and set of frequencies.*

*2.1.3. Procedure*

Dielectric analysis was performed using TA Instruments DEA 2970. For DEA, the sample was placed on a single surface gold ceramic inter-digitated electrode and heated to isothermal temperatures. The procedure includes ramp at $5^{o}C\ min^{-1}$ to $37^{o}C$ and held isothermal for 45 minutes with a flow rate of 50 ml $min^{-1}$ in nitrogen. Shedded snake skin, a black snake skin (and pig skin were used in this study as a barrier for the transport of insulin using an AC electric filed. DEA measures the electrical properties of the drugs used in this study as a function of time, temperature, and frequency. Ionic conductivity was then measured as a function of DEA variables to obtain permittivity [e'], dielectric loss [e''] and loss tangent [tan delta=e''/e']. Permittivity is proportional to the capacitance and measures the number of dipoles. Loss factor is proportional to the

conductance and represents the energy required to align dipoles and move ions by the hopping model (Polaron theory). Ionic conductivity relates to the viscosity of the sample because fluidity is identified by the ease with which ionic components can migrate through the sample under the applied electric field.

## 2.2 Differential Scanning Calorimetry

Differential Scanning Calorimetry (DSC) is a thermoanalytical technique which measures the difference in heat flow rate between a sample and reference as a function of temperature. Both the sample and reference pans are maintained at nearly the same temperature throughout the experiment. Differences in heat flow occur due to the heat capacity of the sample which increases with temperature. The fundamental principle underlying this technique is that, when the sample undergoes a physical transformation such as phase transitions, less or more heat must flow to the sample depending on whether the process is exothermic or endothermic. When less heat is required to raise the sample temperature, there is a result of release of heat which results in exothermic transitions. Crystallization and decomposition involves exothermic process. When more heat flow is required to the sample to increase the temperature at the same rate as the reference heat is absorbed resulting in endothermic transitions. Melting, glass transition, and evaporation involve endothermic process.

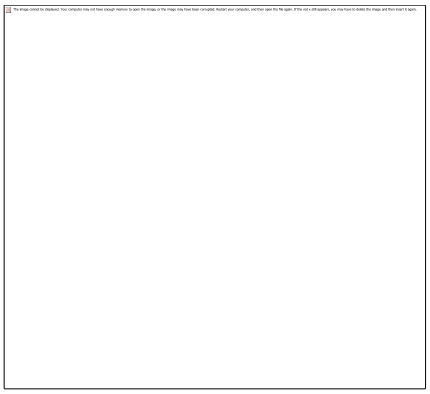

***Figure 3:*** *TAI DSC 2920*

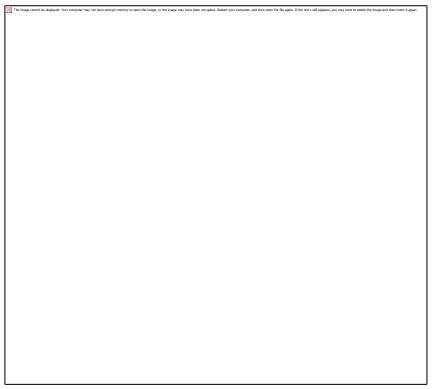

***Figure 4:*** *Mettler DSC 823$^e$ 20*

DSC is widely used in the Pharmaceutical industries to characterize the drug compounds in order to define processing parameters. The amorphous form of the drug is a more efficient drug delivery material and is more bioavailable, but is less stable. It is desirable to process the drug at temperatures below those at which crystallization can occur. DSC also helps in providing changes in the water distribution correlated with the water and solute interactions in a solvent. Application of DSC with respect to Pharmaceutical drugs and chemicals include melting temperature ($T_m$), Glass Transition temperature ($T_g$), Glass transition size, crystallization temperature ($T_c$), crystallinity ($Jg^{-1}$), and Polymorphic Transitions (Figure 5).

***Figure 5:*** *Transitions in a DSC Curve*

*2.2.1 Instrument*

The TAI DSC 2920 and Mettler DSC 823$^{e}$ were used to measure the heat flow properties of pharmaceutical drugs as a function of time and temperature. The experimental parameters like sample size, environment, heating rate and pan type (open pan, closed pan etc.). Solid Fat Index aluminum pans (Figure 6) are used in this study. Sampling size can vary ranging from 2 mg to 15 mg, heating rates ranging from $1^{o}C\ min^{-1}$ to $100^{o}C\ min^{-1}$. The performance of DSC is dependent on all these experimental variables.

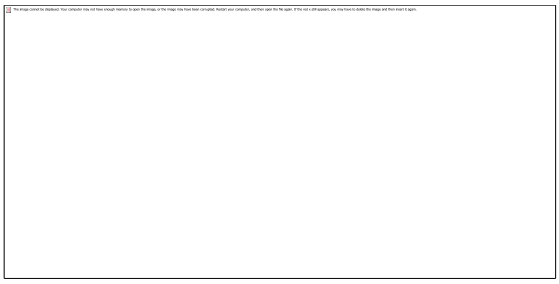

***Figure 6:*** *Solid fat index (SFI) pans used for DSC; left- pan, right- lid*

DSC operates over a temperature range of -100 to +300$^{o}$C for pharmaceuticals. DSC plots are obtained as the differential heating flow (in units of watts sec$^{-1}$, joules sec$^{-1}$ or calories sec$^{-1}$) with respect to temperature. Purge gas; typically Nitrogen (sensitivity) or Helium (resolution) is used at a flow rate of 50 mL min$^{-1}$ and liquid nitrogen cooling when going below the room temperature.

*2.2.2 Calibration*

Calibration of the instrument is essential to have better consistency in results obtained. DSC instrument calibration involves Differential Heat Flow, Temperature and Baseline. Following the ASTM E968 method [4], Differential heat Flow is calibrated. The characteristic temperatures and the enthalpy associated with a phase change of the standard were compared to the literature values [7,8] (Figure 7). Heat flow calibration should not change with heating rate.

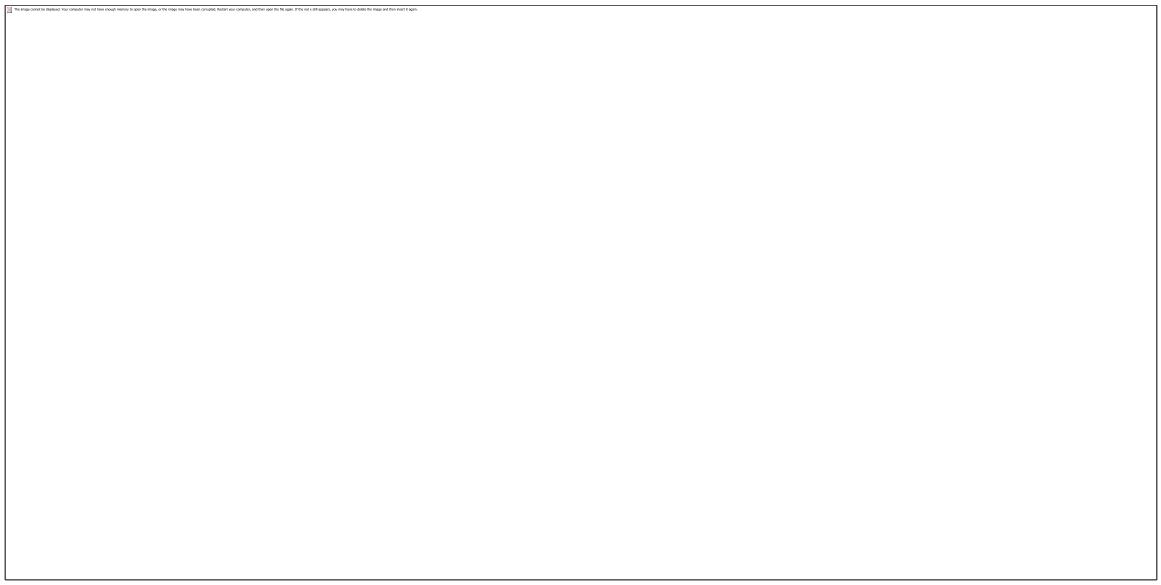

***Figure 7:*** *Differential Heat Flow calibration curve for Acetophenetidine showing Tm and Tmp*

Following the ASTM E967 protocol [5], the temperature of the instrument is calibrated. High purity calibration standards such as Indium, Acetanilde [7] and Acetophenitidine [8] are used for the calibration. DSC Baseline Slope is also calibrated.

*2.2.3 Sampling*

Sample shape, size and weights are to be considered during the packing of sample in the aluminum pan for the DSC run. Sample should be as thin as possible, distributed throughout the pan to have good thermal contact and cover as much of the pan bottom as possible. The thin solid sample can be obtained by cut rather than crushed. A liquid sample is placed in contact with the aluminum pan. A consistent DSC curve can be obtained if there is a good thermal contact of sample with the base of the pan. The experiment can be conducted with an open pan, covered pan or sealed pan and the pan can be either a standard pan which has a flat base or a SFI pan that has crimped base and the reference pan with similar configuration. Crimped pans always have the highest

sensitivity and resolution. The sample size can vary ranging from 2 mg to 15 mg and should be weighed before and after the experiment to observe any mass loss upon heating.

*2.2.4 Procedure*

Calibration of the instrument is the initial step and was performed by following the ASTM standard protocol. Samples were weighed and placed in a SFI aluminum pans with sampling size ranging from 2 mg to 15 mg. Open and closed pans were used in this study depending on the nature of the sample e.g. solid or liquid. The samples were cooled from 25 to -50$^{\circ}$C and then heated to 120°C at 5$^{\circ}$Cmin$^{-1}$ heating rate with nitrogen gas purge of 50 mL min$^{-1}$ for the study of liquids. Samples were heated to 30$^{\circ}$C above the melting point for solids to see the endothermic process and cooled to 50$^{\circ}$C below the melting point to see the exothermic crystallization process. A DSC scan usually provides the following thermal properties: the Heat of Fusion ($\Delta H_f$), melting temperature ($T_m$), a peak melt temperature ($T_{mp}$), Heat of Crystallization ($\Delta H_c$), crystallization temperature ($T_c$), a peak crystallization temperature ($T_{cp}$), Heat of Vaporization ($\Delta H_v$), vaporization temperature ($T_v$) and a peak vaporization temperature ($T_{vp}$).

**2.3 Thermal Gravimetric Analysis (TGA)**

Thermogravimetric analysis (TGA) or Thermogravimetry (TG) is a thermoanalytical technique used to determine changes in weight of a sample as a function of temperature or time (isothermal TG). A sample of exact weight is heated in a special instrument at a given rate ($^{\circ}$Cmin$^{-1}$) through a measured mass loss attributed to either of the following: dehydration, solvent or solute desorption, a gaseous product formation from a reaction e.g. loss of carbon dioxide from calcium carbonate with a residue of calcium oxide or

decomposition of the sample. Such analysis relies on a high degree of precision in three measurements: weight, temperature, and temperature change.

***Figure 8:*** *Thermogravimetric Analyzer*

The first derivative of the weight vs. temperature curve (DTG) highlights key transitions or changes in the sample more definitively for enhanced interpretation. TG is typically employed in research to characterize pharmaceuticals, chemicals, biological entities or polymers. Combining TG with DSC measures endothermic processes a function of temperature or time in a controlled atmosphere. The data obtained differentiates endothermic and exothermic transitions with no associated weight loss (e.g., melting and crystallization) and those that involve a weight loss (e.g., degradation).

*2.3.1 Instrument*

A TA Instruments Hi-Res TGA Model 2590 TG analyzer was used in these studies. It consists of a high-precision balance with a pan loaded with the sample. Regular heating of furnace and the sample holder up to 800°C in air for 10-15 minutes should be done to keep them clean from organic residues. The sample is placed in a small electrically

heated oven with a thermocouple to accurately measure the temperature. The atmosphere may be purged with an inert gas to prevent oxidation or other undesired reactions.

*2.3.2 Sampling and Procedure*

The samples were prepared by placing one drop of material on to a pre-tared platinum TG pan. The pan was placed onto the auto-loading mechanism of the TG analyzer and an automated loading sequence was initiated. The sample is placed into a furnace which heats the sample, while measuring the weight of the sample every 0.5 seconds. The TG experimental conditions were: Ramp 10°C per minute to 500°C in nitrogen as purge gas at a flow rate of 50 ml $min^{-1}$. 30-50mg of sample was used in each run. An inert atmosphere, usually high purity dry nitrogen, is purged to prevent oxidation or other undesired reactions. Then the data is analyzed using TA software.

TG rapidly measures changes in weight as a sample is heated and is eventually vaporized. This can be used to create a water loss profile that can show the different temperature ranges in which water and other components of a sample vaporize.

## References


1. ASTM E 2038, “Standard Test Method for Temperature Calibration of Dielectric Analyzers”, West Conshohocken PA, vol 14.02, 2008.
2. Alan Riga and Kenneth Alexander, “Electrical Conductivity Analysis/Dielectric Analysis Differentiates Physical Chemical Properties of Drugs and Excipients”, American Pharmaceutical Review.8, Issue 6, 45-50, 2005.
3. Alan Riga, Shouvik Roy and Kenneth Alexander, “A Statistical Approach for the Evaluation of Parameters Affecting Preformulation Studies of Pharmaceuticals by Differential Scanning Calorimetry”, American Pharmaceutical Review.5, Issue 1, 64-72, 2002.
4. ASTM E968-99 Standard Practice for Heat Flow Calibration of Differential Scanning Calorimeters, West Conshohocken PA,
5. ASTSM E967-97 Standard Practice for Temperature Calibration of Differential Scanning Calorimeters and Differential Thermal Analyzers
6. ASTM E 2039, “Standard Test Method for Determining and Reporting Dynamic Dielectric Properties”, West Conshohocken PA, vol 14.02, 2008.
7. CAS no. 103-84-4, Acetanilide
8. CAS no. 62-44-2, Acetophenetidin
9. E473-00 Standard Terminology Relating to Thermal Analysis
10. E691-99 Standard Practice for Conducting an Inter laboratory Study to Determine the Precision of a Test Method
11. E1142-97 Standard Terminology Relating to Thermo physical Properties
12. E1325-02 Standard Terminology Relating to Design of Experiments

# CHAPTER III

# CHARACTERIZATION AND PROPERTIES OF AN ORTHO EVRA®TRANSDERMAL PATCH AND LIDOCAINE BY ISOTHERMAL & SCANNING DEA


## Abstract

An ideal delivery system must include a steady and prolonged therapeutically effective drug concentration with or without minimum side effects. Unique modern methods of drug delivery are turning to transdermal or transoral patches. A great deal of research is being devoted to comprehend and smooth the progress of the growth of a transdermal absorption scheme. The focus of this research is the monitoring of the mobility of drugs and transport properties by Dielectric Analysis. DEA is used to track the drug and drug transport as a function of temperature and frequency. Our first study included characterizing a commercial contraceptive transdermal patch, Ortho Evra® by thermal analytical techniques. The drugs in this product are norelgestromin and ethinyl estradiol. DSC was used to detect any crystalline properties of the two drugs by their melt properties. Having no melting temperatures due to the drugs and detecting a glass

transition suggested that the drugs in the patches were amorphous. If they are amorphous they are more bio-available. DSC also aided in identification of the polymeric adhesive, the polymer backing and the drug properties. The isothermal DEA revealed critical modulating frequencies at body temperature of 460 and 560 Hz for the two drugs.

Lidocaine is an anesthetic prominently used in dental procedures. DSC and DEA properties of Lidocaine have led to a better understanding of transdermal and transoral drug delivery. Lidocaine was evaluated by scanning DSC, isothermal and scanning DEA. Scanning DSC results at the standard heating rate $10^{\circ}Cmin^{-1}$ were Tm 74˚C and Tmp 81˚C. At higher heating rates the melt temperatures were shifted to higher values tm 84˚C and Tmp 89˚C. Heat of fusion was $138jg^{-1}$ and there appears no shift in the values with higher heating rates. Scanning DEA determines the amorphous and crystalline forms of the Lidocaine with respect to temperature. Testing of pure Lidocaine revealed that the amorphous form is several order of magnitude more conducting that the crystalline Lidocaine. Isothermal DEA determined the Critical frequency for Lidocaine transport through the shedded snake skin at a frequency 70 to 100 Hz. This data is critical to the development of an effective transoral patch.

**Key words:** Transdermal patch, Transoral patch, Dielectric Analysis, Critical Frequency, Differential Scanning Calorimerty

## 3.1 Introduction

An ideal delivery system must include a steady and a prolonged therapeutically effective drug concentration with or without minimum side effects. A unique modern method for drug transport is employing a transdermal patch. [1]The market for transdermal drug delivery is over $3 Billion annual, just in the US, with this estimation including only the traditional patch markets such as Lidocaine, Nicotine and Estradiol. This type of patch avoids the chemically hostile gastrointestinal environment, has reduced systemic side effects and sometimes has improved efficacy over other dosage forms [4]. In addition since transdermal patches are user friendly, convenient, painless and offer multi-day dosing, it is generally accepted that they offer improved patient compliance [7].

Ortho Evra®, a commercial transdermal patch has 6.00 mg of norelgestromin and 0.75 mg of ethinyl estradiol as the API drugs. Molecularweight of norelgestromin is 327.47 and that of ethinylestradiol is 296.41. The patch is a thin, matrix-type consisting of three layers: the backing layer, middle layer and the release liner.

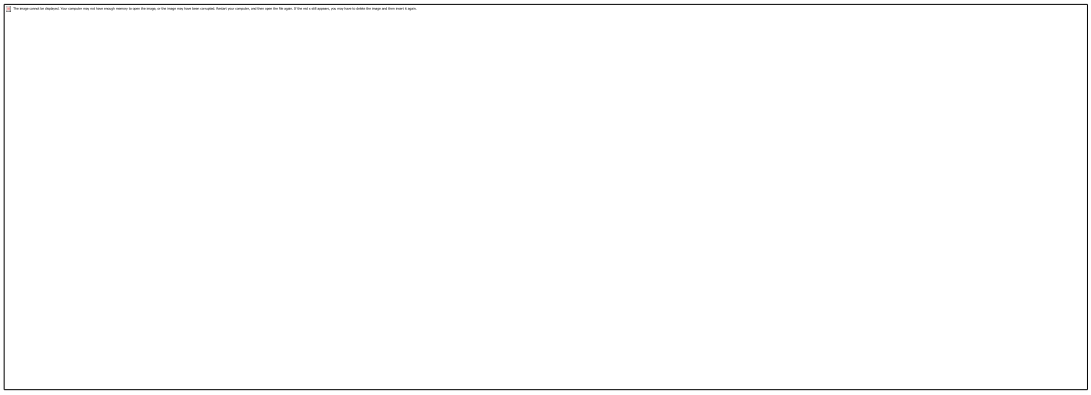

The backing layer is a flexible film which helps in supporting and protects the middle adhesive layer from the environment. It has a low-density pigmented

polyethylene outer layer and a polyester inner layer. The middle layer contains the active components; the two drugs norelgestromin and ethinylestradiol, and the polymer, Styrene Butadiene Rubber (SBR) latex as a low molecular weight resins an inactive components. The third layer is the release liner, which protects the adhesive layer (backing material) during storage and is removed prior to the application of the patch. In this study we determined the DSC and DEA properties of each drug.[5] DSC was used to detect any crystalline drugs by their fusion properties. The research protocol was to determine the Critical frequency of each drug in the patch on a Shedded Snake Skin at body temperature as a function of ionic conductivity and time. DEA determined the ionic conductivity of drugs in the patch since it was our hypothesis that the ionic conductivity was directly related to drug delivery from a transdermal patch.

Lidocaine is a local anesthetic and antiarrhythmic drug. Lidocaine patches are used to relieve the pain of post-herpetic neuralgia. It works by stopping nerves from sending pain signals. Lidocaine is used topically to relieve itching, burning and pain from skin inflammations, injected as a dental anesthetic or as a local anesthetic for minor surgery. Lidocaine molecular weight is 234.34 da.

Lidocaine

Bioavalability of Lidocaine when taken orally is 35% and 3% when used for topical administration. Adverse drug reactions (ADR) of Lidocaine when used as a local anesthetic and administered correctly have rare side effects. Most ADRs associated with lidocaine for anesthesia relates to administration technique [13] and hence a great deal of research is being devoted to comprehend and smooth the progress of the growth of a transdermal absorption scheme. The continued focus of this research is the monitoring of the mobility of drugs and transport properties by Dielectric Analysis. DEA is used to track the drug as a function of temperature and frequency. DEA properties of Lidocaine have led to a better understanding of transdermal and transoral drug delivery. Dielectric relaxation processes [tan delta (loss factor/permittivity) vs. temperature] associated with drug transport/activity in each patch were detected at body temperature. It appears that the DETA properties are related to drug diffusion from the polymeric patch through the bio-membrane to the gold ceramic interdigitated sensor.

### 3.2 Experimental Procedures

A TAI 2920 DSC employing a cool-heat-cool cyclic procedure at 10°Cmin$^{-1}$ in Nitrogen with closed-crimped aluminum pan and a typical 5 mg sample size. Lidocaine melt temperature is 74-81$^{o}$C. We also evaluated Ibuprofen with and without the shedded snake skin. The commercial OrthoEvra®, the birth control patch was also evaluated to verify the experimental conditions.

A TAI 2970 Dielectric Analyzer was used with a ramp of 5°Cmin$^{-1}$ in Nitrogen with single surface sensor interdigitated array gold ceramic electrodes were used to

collected electrical properties of the Dentipatch®, USP Lidocaine, and USP Ibuprofen. The TAI 2970 DEA was also set in the isothermal mode at 37$^{o}$C employing a frequency sweep from 0.10 to 10000 Hz for at least 50 minutes. The latter procedure was followed for the Lidocaine crystalline solid by heating the sample through the melt to 100$^{o}$C and then cooled to room temperature. A second DEA run of the amorphous drug was initiated and followed the same procedure as in the first run.

### 3.3 Results and Discussion

The DSC evaluation of the Ortho Evra® commercial patch revealed a low temperature Tg at -29˚C. It is our interpretation that the Tg is due to a pressure sensitive adhesive with a tackifier, typically used currently in commercial patches. [14] Usually the polymer is Styrene Butadiene Rubber (SBR) latex as a low molecular weight resin. The melting characteristics at higher temperatures were identified as the polymer backing material of the commercial patch. The melting at 105 to 114˚C was repeated at 109 to 116˚C. This material was isolated and further identified by quench cooling the polymer in liquid nitrogen, -120˚C, and further examined to find that the backing polymer was the only crystalline entity in the patch. Therefore, the drug component was amorphous and more bio-available, Figure 9

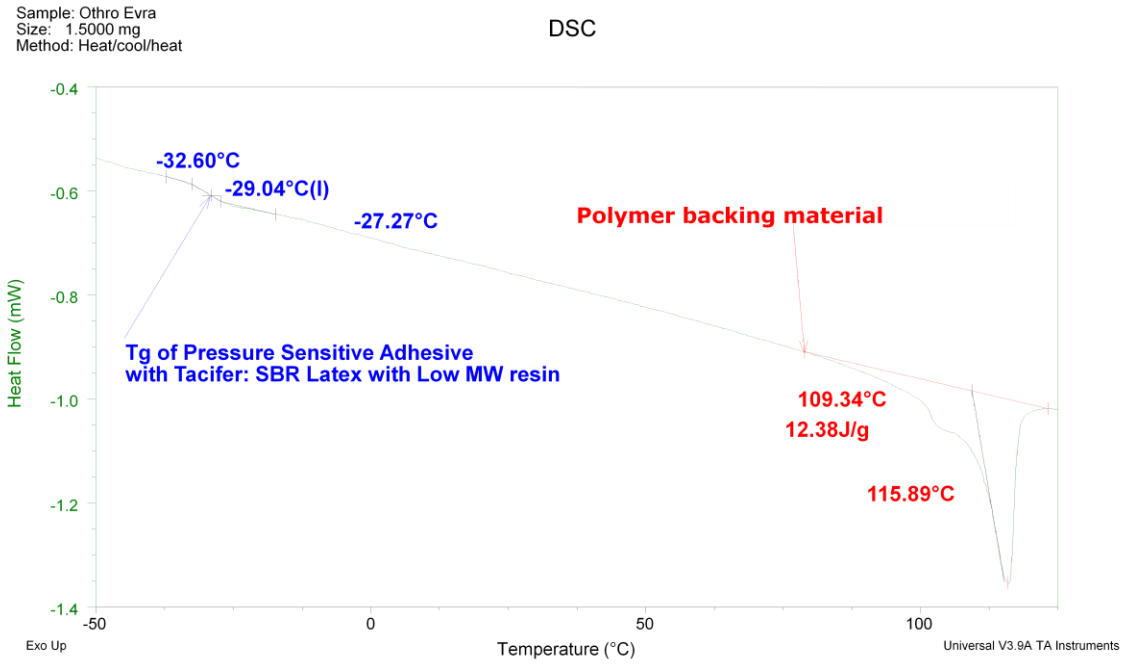


***Figure 9:*** *DSC of OrthoEvra commercial patch*

The scanning DEA produced a conductivity peak vs. temperature for the polymer backing material at 93 to 95˚C. It is interpretated as the DEA melt temperature of low density polyethylene which confirms the DSC results. The peak conductivity temperature was constant with all frequencies and therefore implies that it represents a first order thermodynamic transition as a melt transition, i.e. melt of low density polyethylene. (Figure 10)

***Figure 10:*** *DEA conductivity peak vs. temperature*

The Tan Delta vs Temperature plot yielded a bimodal critical peak response. (Figure 11) The tan delta a Debye plot values, as a function of temperature and frequency at <100˚C revealed a number of polarization processes due to the two drugs. It was assumed that the lower four critical peak frequencies occurring at lower temperatures and the three critical peak frequencies occurring at higher temperatures were taken both as a different set of values. Our proof of concept was the plot of log peak frequency vs reciprocal temperature ($K^{-1}$) would have a statistical correlation coefficient of >0.95. We observed for the lower temperature critical peaks the $R^2$ was 0.98 (Figure 12) and $R^2$ for the higher temperature critical frequency peaks was 0.99 (Figure 13). These curve fits were then used to determine a critical frequency at 37˚C by extrapolation for the two drugs. Based on the functional group analysis and evaluation of the dielectric constant of the two drugs

we assumed the lower peak frequency values were associated with ethinyl estradiol and high peak frequencies were that of norelgestromin. The results are 460 Hz for ethinyl estradiol and 562 Hz for norelgestromin. These critical frequency determinations were confirmed by plotting Log ionic conductivity vs time and then determining the log conductivity vs log frequency at 37˚C and at a time period of 20 min (Figure 14). The deviation in this latter plot was determined and found to be within 10% the same values for the first method to determine the critical frequencies for aiding drug delivery; both methods gave critical frequencies of ca. 500 to 600 Hz to push the drugs from the patch into skin. The isothermal DEA revealed a critical modulating frequency at body temperature.

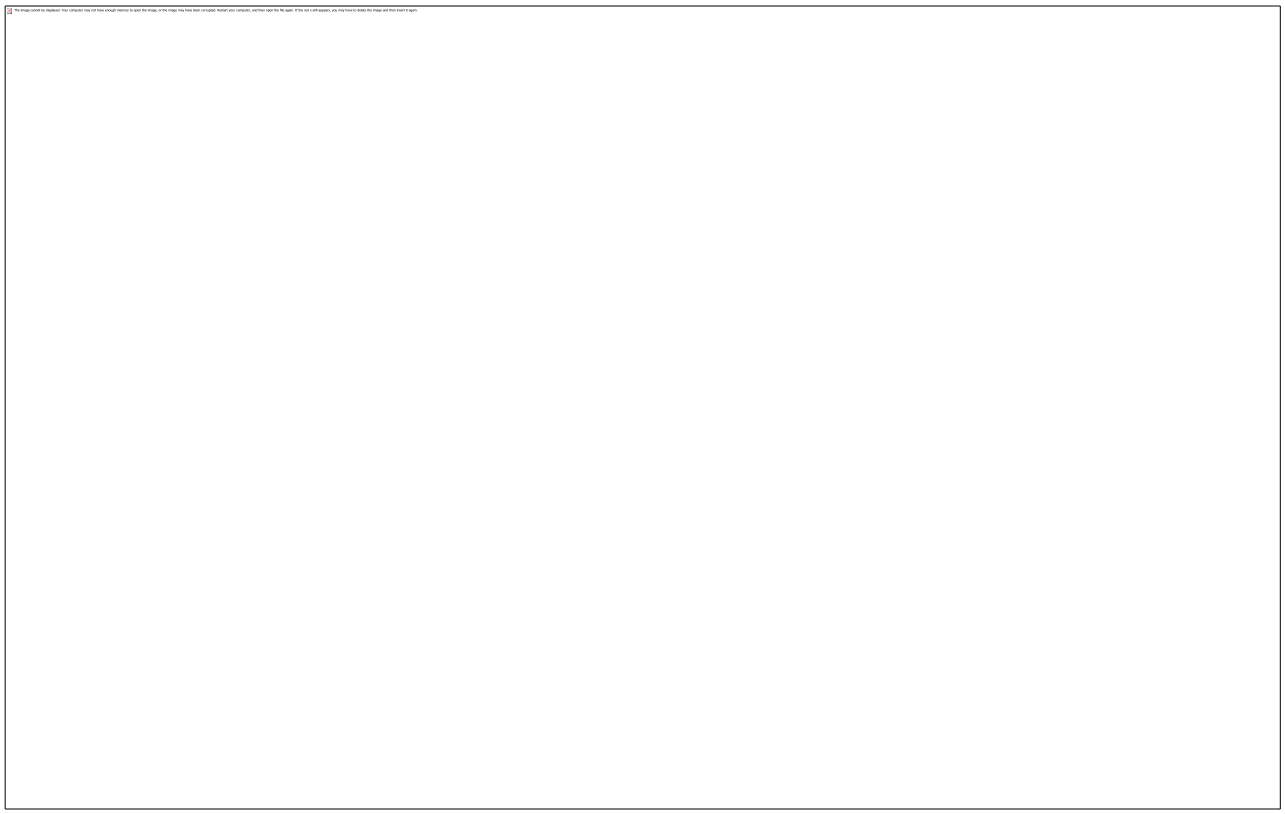

***Figure 11:*** *Tan Delta vs Temperature plot bimodal critical peak frequencies*

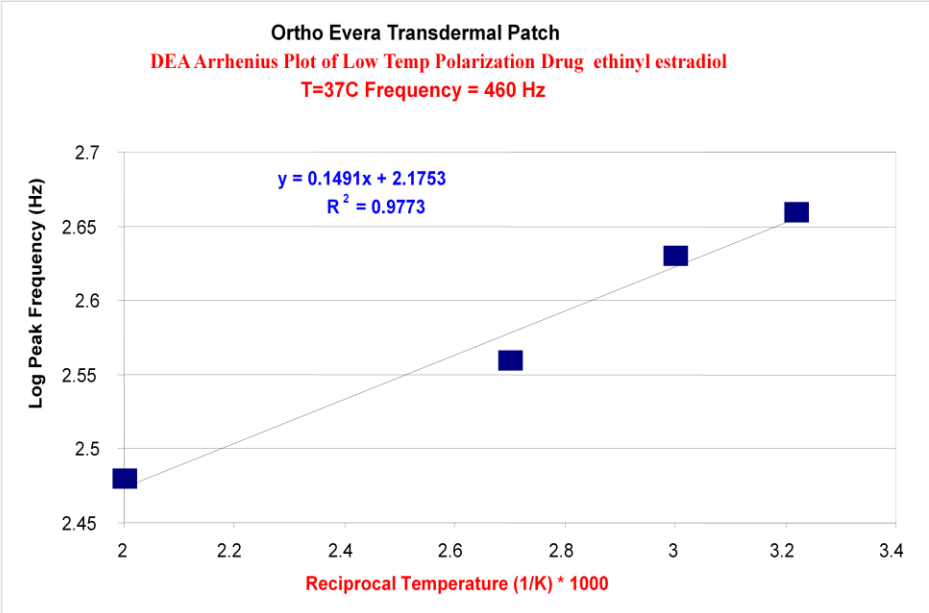


***Figure 12:*** *log peak frequency (Hz) vs reciprocal temperature ($K^{-1}$)*

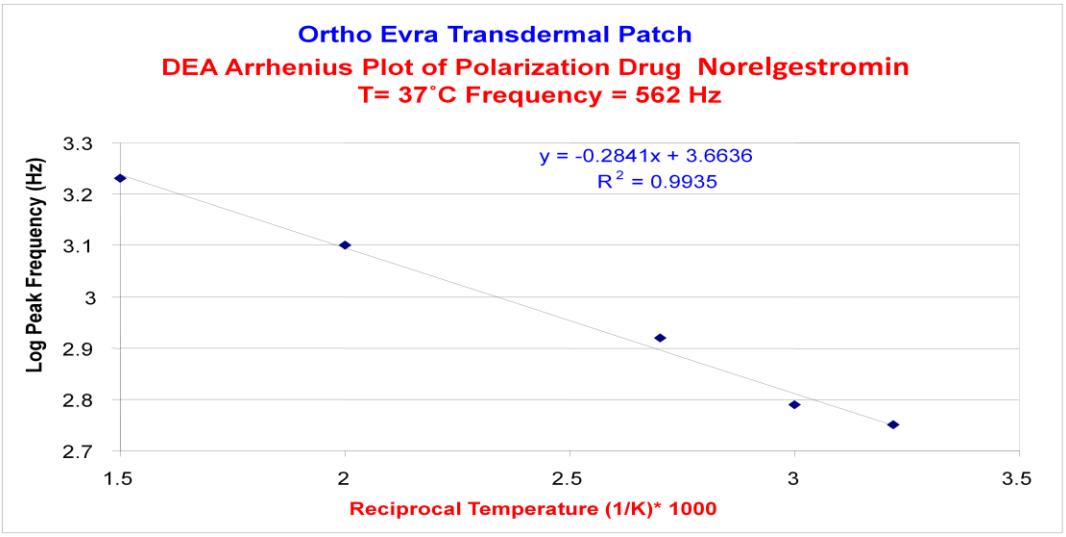


***Figure 13:*** *log peak frequency (Hz) vs reciprocal temperature ($K^{-1}$)*

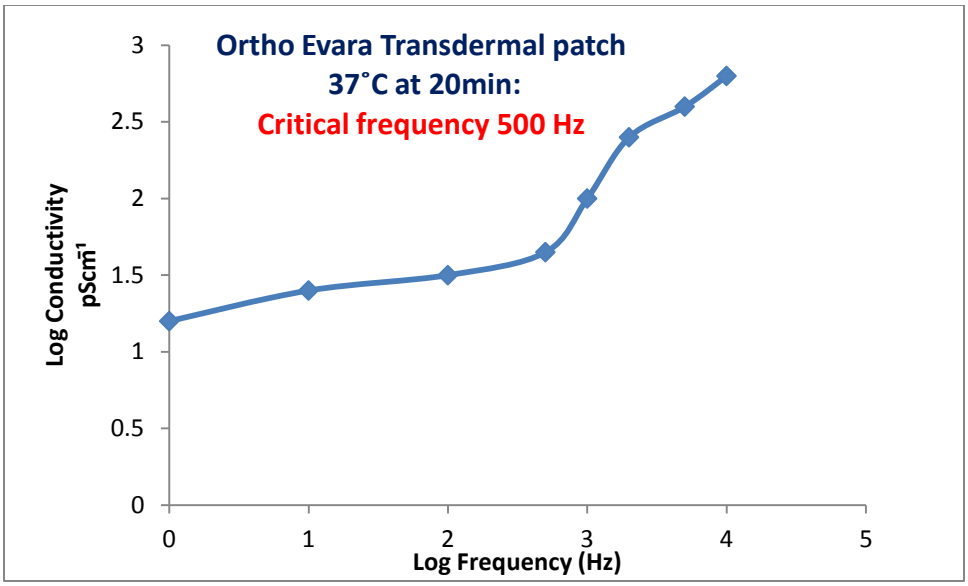


***Figure 14:*** *Log Conductivity (pScm¯¹) vs Log Frequency (Hz) Ortho Evra patch*

Lidocaine, an analgesic, was also examined by DSC and DEA. The melt profile as a function of heating rate is disclosed in Figure 15. The DSC results at the standard heating rate 10˚Cmin$^{-1}$ were $T_m$ 74˚C and the $T_{mp}$ is 81˚C. However, when the heating rate was increased to 75 or 100˚Cmin$^{-1}$ the $T_m$ was 84˚C and the $T_{mp}$ was 89˚C for both higher heating rates. The heat of fusion was 138 Jg$^{-1}$ for the standard rate and 135, 144 Jg$^{-1}$ for the higher rates. Only the $T_m$ and $T_{mp}$ increased but the heat of fusion appears to be the same.

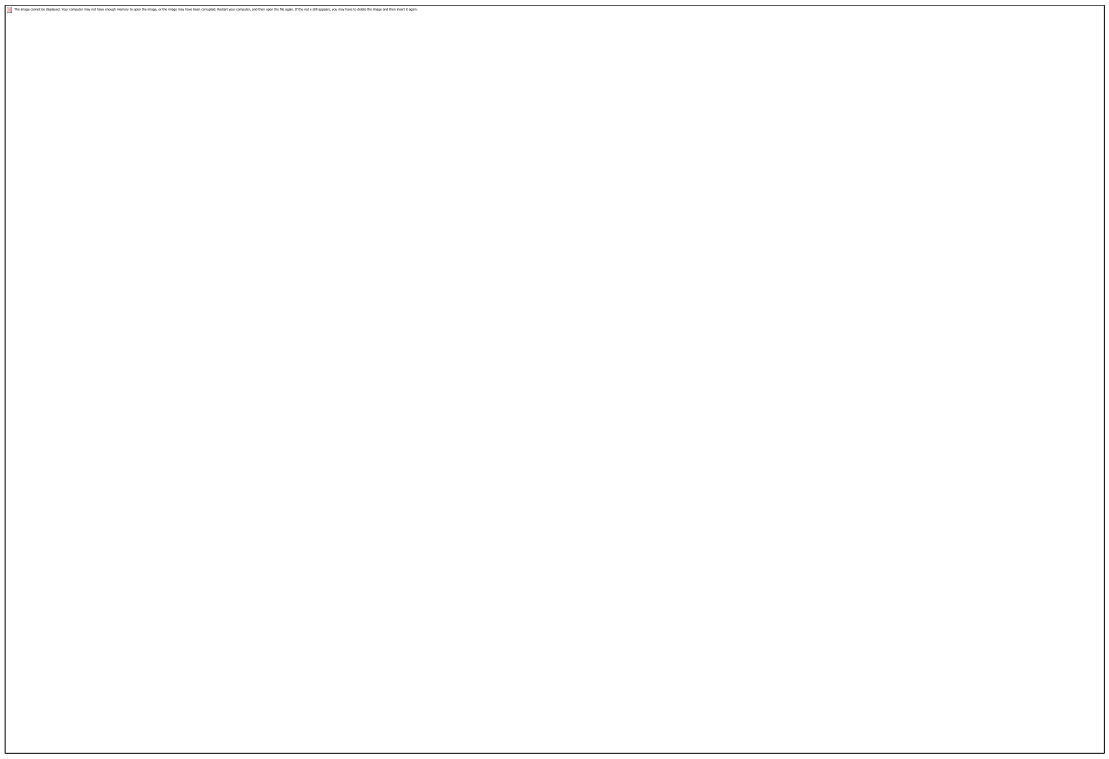

***Figure 15:*** *DSC of Lidocaine with higher heating rates*

The DEA curves of log ionic conductivity vs. temperature for Lidocaine or Lidocaine.HCl were definitive in that the first run depicted a crystalline material, its solid state with an initial ionic conductivity of $10^{-1}$ $pScm^{-1}$ at $50^{o}C$. The melt properties as a function of frequency were $10^{5}$ to $10^{6}$ $pScm^{-1}$. The second run was clearly an amorphous chemical with the initial ionic conductivity starting at $10^{4}$ $pScm^{-1}$ at $50^{o}C$ and in the melt $10^{6}$ $pScm^{-1}$. The HCl salt of Lidocaine and the Lidocaine without the salt was observed to have the same results.

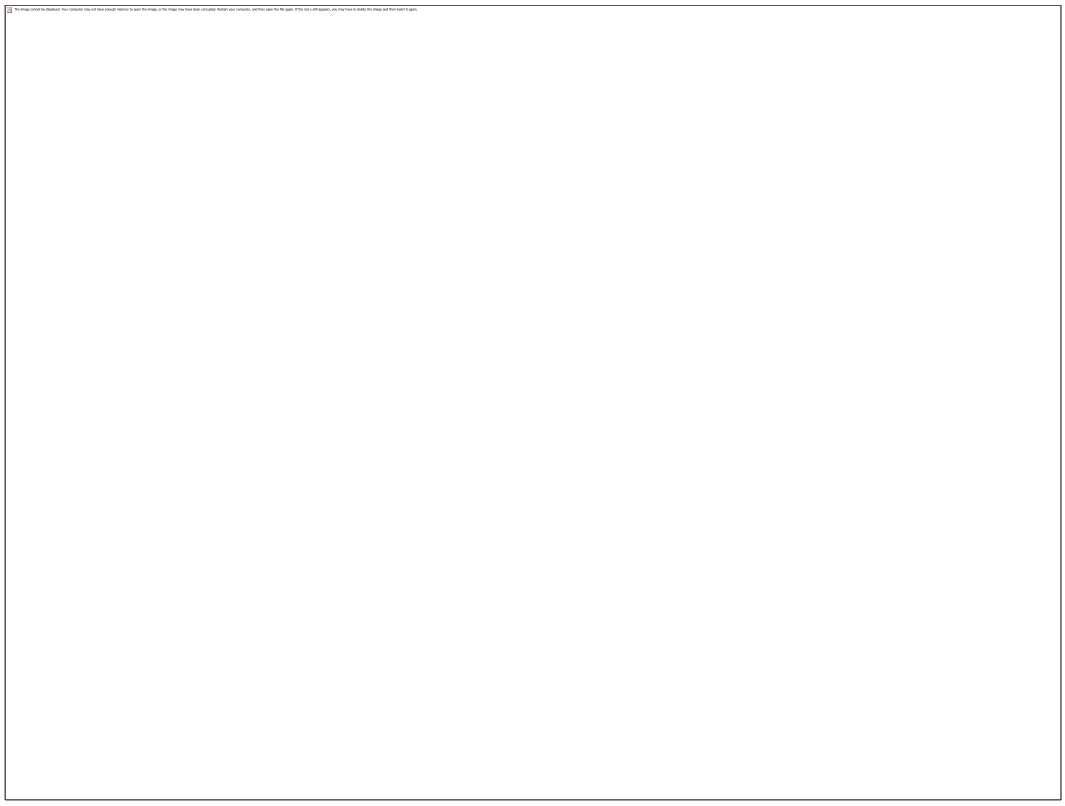

***Figure: 16*** *Lidocaine Hcl Ionic Conductivity vs. Temperature*

An alternative technique to determine the **critical frequencies** needed to manipulate the drug and push it through a bio-membrane for DEA drug transport was developed. First, plot log ionic conductivity vs. time and vary the frequency at a given temperature. At a set time of 20 min. record the log ionic conductivity vs. log frequency. Evaluate this last plot for significant change as an increase (the ionic drug is transporting through the membrane) or decrease (the drug has completely transported through the membrane) in the conductivity and note the critical frequency at the start of the variation. This initial frequency variation is the "**critical frequency".** The critical frequency for Lidocaine or Lidocaine.HCl was 70 to 100 Hz. This method of analysis for the critical frequency was tested by evaluating a drug on a shed snake skin bio-membrane and determining the effective drug through put by a calibrated UV analysis.

***Figure 17:*** Lidocaine *Log ionic conductivity vs. time*

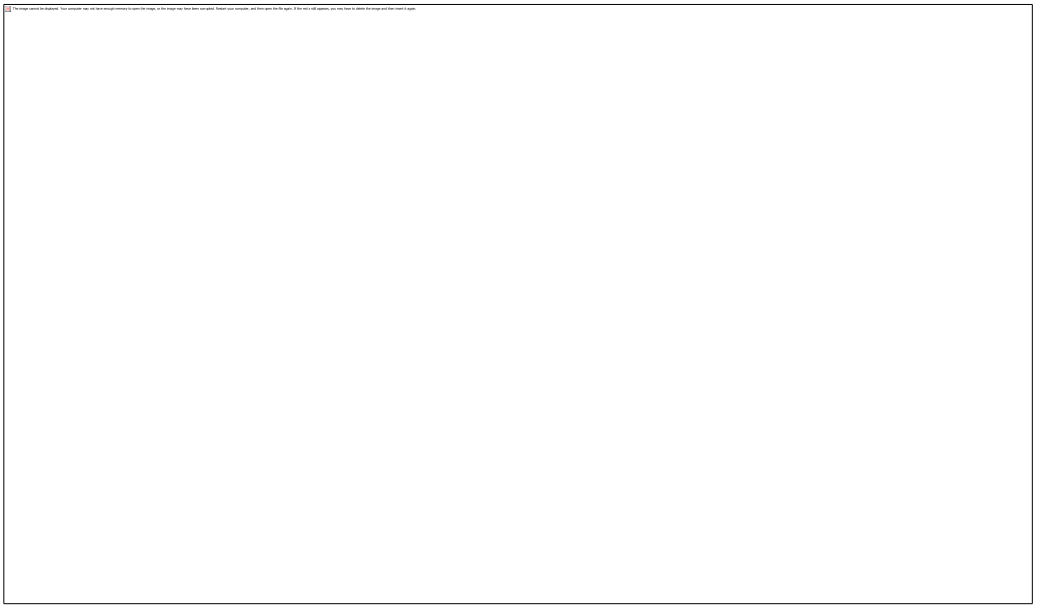

***Figure 18:*** *Lidocaine Log conductivity vs log frequency*

From the plot of log ionic conductivity vs. log frequency for a crystalline Lidocaine vs. an amorphous Lidociane, one observes clearly that the amorphous form is more conducting than the crystalline form, which is a well known observation. (Figure16)

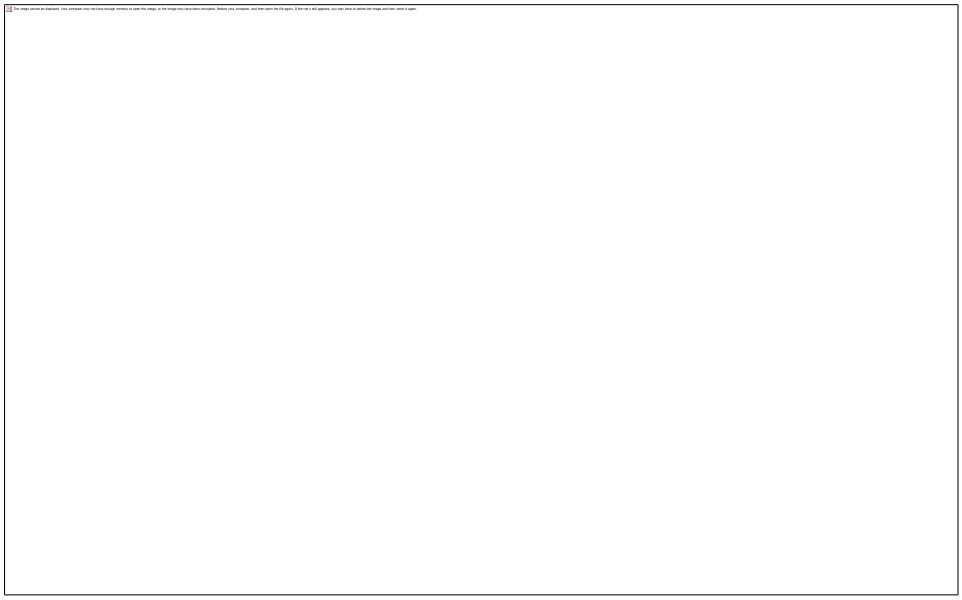

***Figure 19:*** *Log Conductivity vs. log frequency of amorphous and crystalline form of Lidocaine*

### 3.4 Conclusions

Having no melting temperatures due to the drugs, however a melting process due to the backing polymer polyethylene and detecting a glass transition suggested that the drugs in the patches were amorphous. If they are amorphous they are more bio-available. Drug DEA properties proved appropriate in evaluating transdermal & oral patch drug delivery as monitored by Ionic Conductivity. One can scan or ramp temperature employing DSC and DEA to study the transdermal or oral patch for its components e.g. the polymeric adhesive, the polymer backing material and the active ingredient, the drugs. Alternately one can scan for the effect of the drugs by DEA at isothermal $37^{o}$C, that is, measure the

ionic conductivity vs. temperature and frequency range (0.1 to 5000 Hz). Unique dielectric properties of the Ortho Evra® patch have been determined. One can modulate drug distribution [increase its transport through the shedded snake skin] at >600 Hz at body temperature. The critical frequency for the commercial patch was based on the DEA Tan Delta vs. Temperature and frequency plots using the Arrhenius Model. For Lidocaine, the modulating drug distribution frequency is at 100 Hz based on the isothermal DEA 37$^{o}$C Conductivity vs. Temperature and Frequency. Transdermal and Trans-oral patch drugs are amorphous and drug transport monitored by ionic conductivity is enhanced over the crystalline drug as discovered when characterizing an Ortho Evra® patch and Lidocaine on a model skin, shedded snake skins.

## References


1. R.O. Potts and R.H. Guy, Editors, “Mechanisms of Transdermal Drug Delivery”, Marcel Dekker, New York, 1997, 1-350.
2. A. Naik and R.H Guy, “Infrared Spectroscopic and DSC Investigations of Stratum Corneum Barrier Function”, in “Mechanisms of Transdermal Drug Delivery, Potts and Guy Editors, M. Dekker, NY, 1997, 87-162.
3. R. Burnette and J. D. DeNuzzio, “Impedance Spectroscopy: Applications to Human Skin”, in “Mechanisms of Transdermal Drug Delivery”, Potts and Guy Ed, M. Dekker, NY, 1997, 215-230.
4. A. Riga, J. Cahoon and L. Lvovich, “Characterization of Organic Surfactants and Dispersants by Frequency Dependent Electrochemical and DEA Techniques”, ASTM STP 1402, 2001, 157-173.
5. A. Riga, G. Pan, R. Macedo and K. Alexander, “Characterization and Analysis of Pharmaceuticals Part One, Multiple and In-Tandem Thermal Analysis Techniques”, American Pharmaceutical Review, 6, Issue 1, 2003, 110-114.
6. A. Riga, G. Pan, and K. Alexander, “Activity of Drugs in Transdermal Patches by DEA”, Proceedings of the NATAS, 30, 2002, 102-105.
7. T. Kinoshita, etal, “Transdermal delivery of Lidocaine in vitro by alternating current” , J. Med. Dent. Sci., 50, 71-77, 2003.
8. A. Riga, K. Alexander and K. Bhasi, “Characterization of Snake Skins by Thermal Analysis”, JTAC, 75, 269-276, 2004.

9. T. Pongianyakul etal. “Shed King Cobra and Cobra Skins as model membranes for in-vitro nicotine permeation studies”, J. Pharmacy and Pharmacology, 54, 1345-1350, 2002.
10. D Jackson, AH Chen, and CR Bennett (1994). "Identifying true lidocaine allergy". *J Am Dent Assoc* 125 (10): 1362–1366.PMID 7844301.
11. T. Kinoshita, etal, “Transdermal delivery of Lidocaine in vitro by alternating current , J. Med. Dent. Sci., 50, 71-77, 2003.

# CHAPTER IV

# THERMAL AND BIO-ANALYTICAL CHARACTERIZATION OF AQUEOUS DRUGS AID THE DEVELOPMENT OF DRUG DELIVERY IN ANIMAL MODELS


## Abstract

Transdermal drug delivery has many benefits over systemic oral therapies, in which clinically sufficient quantities of the active pharmaceutical ingredient do not reach the intended organ and/or use of the drugs result in serious side effects. However, existing transdermal platforms are limited to drugs of small size, ionic nature and low molecular weight. In the case of diffusion, treatment time is passively determined by the typically slow diffusion process rather than the therapeutic need. An optimally-tuned low-voltage applied AC electrical field has been found capable of inducing polarization and delivering micro- and macromolecules through a biological membrane. In this study, insulin, Diphenhydramine and Lidocaine gel were transported by AC electrokinetic's through animal models, including pig skin and shedded snake skin at body temperature. A factorial design was used to establish experimental parameters for the insulin solution evaluating variables of voltage, frequency, time, temperature, drug dose, and membrane thickness. Pre- and post-test conductivity measurements of the pig skin samples are taken

as an indicator of drug permeation and changes in conductivity are correlated with experimental variables to assess the relative importance of each variable to drug transport. Dielectric Analysis was used to modulate the drugs delivery response measured by a change in the log conductivity vs. log frequency curve at lower frequency of 500Hz and a higher frequency of 1000 Hz for insulin at 37ºC. Proof of concept for the drug transport was confirmed by examining a residue on the electrode by Ultra Violet Spectroscopy. Lidocaine gel and Diphenhydramine as formulated drugs, in an aqueous solution were also evaluated by the AC field to determine their transport performance. A clear result of the experimental design for insulin was that the low frequency was significant in enhanced drug delivery. Imposition of a low frequency of 500Hz aliened dipoles and higher frequency aided the mobility of the drug ions into the bio-membranes.

**Key words**

Transdermal drug delivery, Dielectric Analysis, UV Spectroscopy, Lidocaine gel, Diphenhydramine, insulin, AC electrokinetics, polarization

## 4.1 Introduction and Background

Advances in biotechnology, particularly in recombinant protein technology, lead to a great deal of attention to the therapeutic roles of peptides and proteins. Protein and peptide drug delivery has been an area of intensive research because of their efficacy in several disease conditions [1]. Most protein and peptide drugs are currently used as parenteral formulations because of their poor oral bioavailability and they do not reach the target organ either fast enough or in high concentrations when delivered via other routes [3]. These drugs are usually recommended for chronic conditions, and the use of injections on a daily basis during long-term treatment has obvious drawbacks [9]. Insulin is the most important among the therapeutic proteins and peptides being explored. About 2 million American people are suffering from hyperglycemia which requires insulin for the treatment. Exogenous insulin administration is basically a replacement therapy, when administered subcutaneously yield a plasma profile which mimics the endogenously secreted insulin in a normal individual. There is extensive research on several aspects of the insulin delivery. In recent years, there has been a great deal of interest in the exploitation of non-invasive routes for insulin therapy, and their development by the pharmaceutical industry, including oral, nasal, buccal, pulmonary, transdermal, rectal, and ocular drug delivery systems [16]. The transdermal patch delivery system presents distinct advantages over systemic drug delivery in reducing the problem of hyperinsulinemia[15, 16]. This new delivery system reduces the chance of micro and macro angiopathy, infection and pain as well as improving patient compliance. Injection dosing also has specific advantages as efficacy. The problems with injections include: restricted fat deposition at the injection site, which leads to local hypertrophy, inability to

load the syringe and administer it as well as the pain, cost and infections [21]. Therefore, the transdermal dosing remains a better route for drug administration.

Compared to other means of drug delivery, the transdermal route offers unique advantages: transdermal drug delivery is non-invasive; absorption is not affected by food intake and is not subject to first-pass metabolism in the liver [11]. In addition, active transdermal drug delivery systems allow precise control of drug dosing [10]. However the drug delivery is enhanced through modulation of an electric field (Dielectric Transdermal process) used to drive drug transport [4]. All transdermal drug delivery methods introduce therapeutic agents into the body through the skin. Drug transport can either be passive, relying on drug diffusion across the skin, or actively driven by application of an electric field [8]. The drug delivered, aided by an electric field, had appropriate pharmacokinetics and pharmacodynamics, and the drug was stable in the patch. Depending on the drug in the patch the time duration of delivery can be up to 1 to 7 days.

Electrically-assisted transdermal delivery is the facilitated transport of compounds across the skin using an electromotive force. Depending on the nature of the applied electric field, the molecule to be delivered and the barrier to be crossed, various combinations of the driving forces such as iontophoresis, electrophoresis (EP), electroosmosis (EO), dielectrophoresis (DEP), and others are used. Electrophoresis and dielectrophoresis using alternating current (AC) and iontophoresis using a direct current (DC) may be described as the electrically assisted movement of chemicals and molecules through the membrane during the application of an electrical potential difference. These techniques have been widely used in various medical fields, including topical and

systemic drug delivery systems. In particular, the effectiveness of transdermal delivery using electrokinetics for the administration of topical anesthesia and analgesia has been widely reported reference. Another advantage of electrokinetic methods is the ease of interpretation and characterization by Electrochemical Impedance Spectroscopy (EIS) based sensors and detection methods. EP and DEP in combination with EIS can effectively trap, manipulate, separate and quantitatively detect particles ranging from virus to large DNA strands, to bacteria and mammalian cells in micro fabricated devices.

Typically interdigitated electrodes and Microelectromechanical systems (MEMS) technology are used because they are easy to fabricate, can generate strong electric fields with a reasonable voltage, work optimally with micro scale particles, integrate seamlessly with micro fluidics, and have analytical electric field solution available for modeling. Electrochemically iontophoresis enhanced transdermal patches are often constructed with one active or "donor" electrode and one counter or "acceptor" electrode which are placed close to each other and directly against a tissue barrier (stratum corneum). The delivered drug is attached to the donor electrode as a medication soaked sponge or gel. In DC iontophoresis, a constant current or voltage is applied between the electrodes to promote transport of a drug from the donor electrode to the acceptor electrode through the tissue barrier, which is assumed to be a path of least resistance between the two electrodes. In practice this is usually not the case, often resulting in a very low percentage efficiency of the drug delivery through the tissue barrier. In DC iontophoresis the rate of drug delivery increases with the current and maintaining a high current (in the 1 mA range) by applying high DC voltage is desirable. However, these high currents present risks to patients in the clinical setting (a current of 10mA can stop pace maker)

where the acceptable limit for a DC application is 10 μA. A number of adverse effects have as a result of high applied voltages, including electric burns or erythema;[6] have been reported for treatments involving DC iontophoresis. The application of DC-based electrokinetics methods has been limited to a period of approximately 15 minutes. The attempt was made to operate at higher frequencies (electrophoretic delivery at ~ 100 kHz) where the high current threshold increases to 1 mA. However, this approach results in uncomfortably long treatment times on the order of hours. Therefore, iontophoresis is typically limited to low DC voltages in order to avoid potentially dangerous high currents, resulting in a long treatment time (order of hours) required to achieve any sizeable drug transport. However, even for longer treatment times, the amount of transported molecules is very small, and therapeutically insufficient in the majority of applications. The main goal of this study is to investigate various variables and optimize the conditions such as length of treatment and low currents for effective transdermal drug delivery of macromolecule e.g. insulin.

## 4.2 Experimental Materials and Procedures

### *4.2.1 Biological tissue membranes and Drug selection*

In this study selected biological tissue membranes- excised pig skin of 1-3mm thickness and shedded snake skin of 1 mm thickness were used to investigate electrokinetic drug transport. These skins serve as early stage models for transdermal drug delivery in humans. Pig skin was stored in a plastic bag in the refrigerator at -10ºC and shedded snake skin was stored in a plastic bag at 4ºC. The skins were excised and the subcutaneous and fat tissues were removed. The excised skins were composed of stratum

corneum, viable epidermis and upper epidermis. Stratus corneum, the outermost layer of mammalian epidermis, acts as the main barrier for diffusion of substances through the skin.

In this study, Insulin, Diphenhydramine, Lidocaine gel, Nimsulide and JCC 76 with different molecular weights and various polarities were selected as model drug compounds. Insulin is a hormone that is central to regulate the energy and glucose metabolism in the body. Insulin is a peptide hormone composed of 51 amino acids and has a molecular weight of 5808 Da. The interior of insulin contains mostly non-polar amino acid side chains, chains e.g. chain to chain bonding with cysteins which are nonpolar and hydrophobic while the exterior contains mostly polar amino acid side.

***Figure 20:*** *Insulin primary structure*

*4.2.2 TA Instruments Dielectric Analyzer DEA 2970*

Dielectric analysis was performed using TA Instruments DEA 2970. For DEA, the sample was placed on a single surface gold ceramic inter-digitated electrode and heated to isothermal temperatures. The procedure includes ramp at 5ºC $min^{-1}$ to 37ºC and held isothermal for 45 minutes with a flow rate of 50 ml $min^{-1}$ in nitrogen. Shedded snake skin, a black snake skin (figure 21) and pig skin (figure 22) were used in this study as a barrier for the transport of insulin using an AC electric filed. DEA measures the

electrical properties of the drugs used in this study as a function of time, temperature, and frequency. Ionic conductivity was then measured as a function of DEA variables to obtain permittivity [e'], dielectric loss [e'’] and loss tangent [tan delta=e'’/e']. Permittivity is proportional to the capacitance and measures the number of dipoles. Loss factor is proportional to the conductance and represents the energy required to align dipoles and move ions by the hopping model (Polaron theory). Ionic conductivity relates to the viscosity of the sample because fluidity is identified by the ease with which ionic components can migrate through the sample under the applied electric field.

***Figure 21:*** *Shed snake skin*

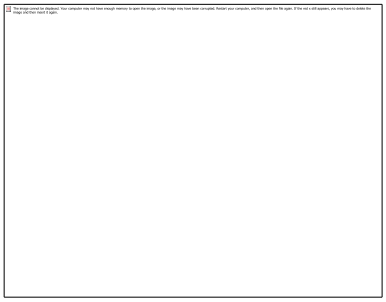

***Figure 22:*** *Pig skin on DEA sensor*

*4.2.3 B-Cell*

The B-Cell (figure 23) was used for initial evaluation of drug transport through biological tissue membranes - pig skin (insulin) and concluded with an experimental design [4]. The selected biological tissue membranes were positioned with the use of several adjusting springs at the bottom of the cell. Then the springs were pressed directly against the "bottom electrode" with the stratum corneum facing the electrode to provide a realistic model of the 5-electrode setup being firmly placed directly against a skin. The biological membranes were sealed properly to avoid cross contamination of the receptor and the donor compartments. The receptor compartment is the bottom side of the

membrane and the donor compartment is above the membrane containing the original drug-containing substance and all the electrodes. The available diffusion area was approximately 4 $cm^2$. Approximately 50 mg samples of the drug-containing substance is placed on the "top electrode" from the above, with some amount of the substance penetrating through the perforation and coming into contact with the biological tissue membrane between the bottom Electrodes 4 and 5. However the majority of the drug-containing substance remains in the perforation holes, between Electrodes 2 and 3 comprising the "bottom electrode", and between the Electrode 1 and the plane of the "top electrode". A capping Electrode 1 covers the sample. All experiments were conducted at $25^0$C.

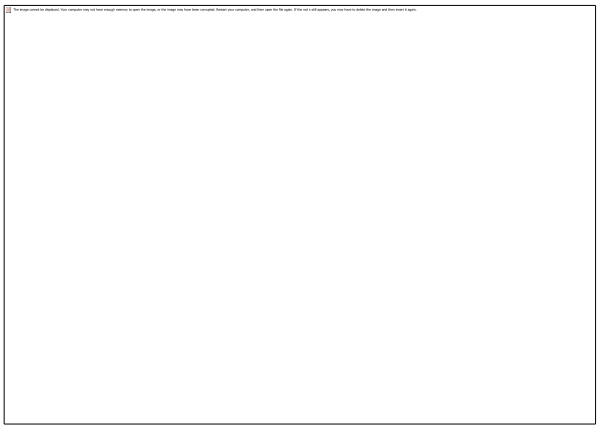

***Figure 23:*** *B-Cell*

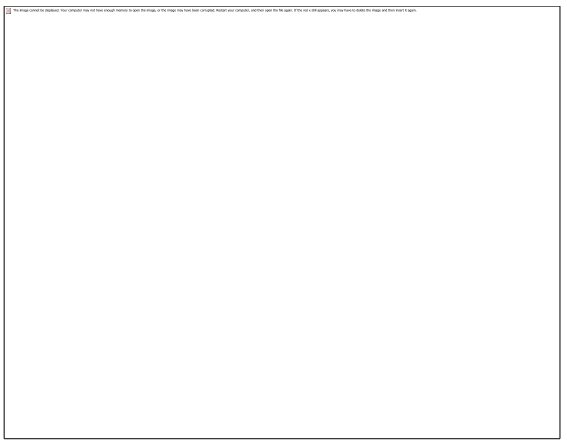

***Figure 24:*** *Interdigitated electrodes*

*4.2.4 Experimental design and statistical analysis*

A series of studies was performed to investigate variables which are important for transdermal transport of drug and changes in the membrane conductivities as a function of voltage amplitudes and frequencies, treatment time, and membrane thickness. This type of factorial design identifies the most important parameters affecting drug transport

such that the parameters can be optimized for effective transdermal drug transportation. The resulting $3^3*2$ factorial design with two variables at two levels and three variables at three levels incorporates a total of 54 studies.

*4.2.5 UV Analysis*

Drug delivery through the membranes was confirmed qualitatively and quantitatively by UV spectroscopy. After completion of the drug delivery cycle the sample in the receptor cell were collected and quantitatively analyzed by UV-Vis spectrometry. The UV-Vis analysis at room temperature was performed and calibration curves of known drug concentrations were developed (Insulin at 271.9nm). After each experiment three aliquots were taken from each solution and each of these was scanned three times. The average of these nine values was used to fit the calibration curve for the peak UV absorbance measurements for the residue samples.

**4.3 Results and Discussion**

*4.3.1 DSC and DEA Results*

4.3.1.1 DSC

The heat of crystallization, heat of fusion and heat of vaporization of unbound water are 334, 334 and 2200 $Jg^{-1}$, respectively. Understanding the role of the solvent (water) on the solute drugs can be accomplished by evaluating and comparing the crystallization, fusion, and vaporization heats of water in the solutions studied. Next, evaluating the crystallization, fusion, and vaporization temperatures we further characterize the solute drug in water. In table 2 and 3 the water analysis of each of the drugs in solutions/gel

revealed that Insulin, Diphenhydramine, and Lidocaine gel crystallized 10˚C above pure water. The melting temperatures were slightly lower than that of pure water and the peak melting temperatures were slightly higher than the water for three drugs. The vaporization properties of water were similar for insulin and Diphenhydramine, however lidocaine gel was significantly difference with a lower amount of water associated to the gel.

| Drug (liquid) | $T_c$ | $T_{cp}$ | $\Delta H_c$ | Relative $\Delta H_c$(%) | $T_m$ | $T_{mp}$ | $\Delta H_f$ | Relative $\Delta H_f$ (%) |
|---|---|---|---|---|---|---|---|---|
| Water | -34 | -30 | 338 | 101 | -1.0 | 2.0 | 373 | 109 |
| Insulin | -25 | -19 | 315 | 94 | -3.6 | 3.1 | 335 | 100 |
| Diphenhydramine | -25 | -18 | 321 | 96 | -2.1 | 4.2 | 345 | 102 |
| Lidocaine gel | -21 | -19 | 200 | 60 | -4.6 | 1.4 | 177 | 53 |

***Table 2:*** *Heat of crystallization and heat of fusion by DSC of various drugs*

| Drug (liquid) | $T_v$ | $T_{vp}$ | $\Delta H_v$ | Relative $\Delta H_v$(%) |
|---|---|---|---|---|
| Water | 99 | 105 | 1998 | 91 |
| Insulin | 102 | 112 | 2056 | 93 |
| Diphenhydramine | 123 | 131 | 1998 | 91 |
| Lidocaine gel | 109 | 111 | 1147 | 52 |

***Table 3:*** *Heat of vaporization by DSC of various drugs*

A calibrated DSC yielded the melting temperature of Nimesulide at 148-150˚C, heat of fusion 54 $Jg^{-1}$, using the TAI DSC 2920 instrument. The literature value for the

melting temperature is 143-144˚C. The crystallization temperature is 104-105˚C and heat of crystallization is 46 $Jg^{-1}$. The ratio of the heat of crystallization to that of heat of fusion is the amount of the re-crystallized drug, i.e. 86% of the drug Nimesulide re-crystallized and by difference 14% is an amorphous form. The melting point of JCC based on the DSC results is 180-183˚C and the heat of fusion is 91 $Jg^{-1}$ (see Figure 25 and 26).

There is no any recrystallization for JCC and hence it is in amorphous form.

***Figure 25:*** *DSC of Nimsulide*

***Figure 26***: *DSC of JCC 76*

4.3.1.2 DEA

DEA was used to monitor in vitro delivery of aqueous solutions and solid forms of drugs. The Interdigitated single surface electrode was used to sense changes in the ionic conductivity as a function of applied frequency at 37$^{o}$C for 45 minutes. Pig skin was employed as the animal model to test the drugs through put with frequency. Figure 27 is an evaluation of pig skin without any drug applied but the effect of varying frequency was measured. The ionic conductivity (pScm$^{-1}$) is plotted against frequency with a linear correlation from log frequency of -1 ($10^{-1}$) to $10^{5}$ Hz. The response fitted a linear curve fit equation of

$$\log \text{conductivity} = 0.668 \log \text{frequency} + 4.92, R2 = 0.998 \quad (a)$$

The insulin test on the electrode produced the next equation see Figure 28.

log conductivity = 0.632 log frequency + 4.62, R2 = 0.996 (b)

The insulin on pig skin is described in Figure 29 to 31 and equation c and d where the curve before the critical frequency of 1.0 Hz is log conductivity = 0.823 log frequency + 5.73, R2 = 0.995 (c ) and after the critical frequency log conductivity = 0.195 log frequency + 7.29, R2 = 0.934 (d).

The interpretation of these curves and equations is that the insulin delivery was enhanced as demonstrated by the slope or rate of charge transfer increase from 0.67 (pig skin only) to 0.82 (insulin on the pig skin) or the ionic conductivity (related to the concentration of the insulin) was enhanced 22%. This template of drug through put is the DEA measure of effectiveness of this DEA technique. The slope or rate of ionic conductivity after the critical frequency decreased to 0.19 and the curve is flat with minimum variation. This is interpreted that the drug was passed through the membrane which will be evaluated by UV analysis of the through put fluid described later in this chapter.

The next aqueous solution with a drug, was with diphenhydramine, and examined the same manner. Figure 32 is the overall measure of log ionic conductivity vs. log frequency from log frequency from $10^{-1}$ to $10^{5}$ Hz, see Figure 33. Immediately seen is an upward movement of the curve at 10 Hz and again at 100 Hz are noted as the critical frequencies for this aqueous drug. The general equation curve fit was in Figure 33

Log conductivity = 0.549 log frequency + 5.85, R2 = 0.901 (e)

An evaluation of the curve by breaking down the range of response in this case to $10^{-1}$ to $10^{1}$ was in order (frequency range prior the critical frequency). This equation is (f) is

Log conductivity = 0.780 log frequency + 5.80, R2 = 0.994 (f)

After the critical frequency of 1.0 Hz is viewed in Figure 35 and equation (g)

Log conductivity = 0.264 log frequency + 6.89, R2 = 0.323 (g)

This set of equations and curves implies that the pig skin slope 0.67 increased to 0.78 or a 16% ionic conductivity enhancement (or a 16% increase in drug through put, which will be tested by UV analysis of the fluid beneath the pig skin. The slope after testing was 0.26 a decrease from 0.78 before the critical frequency. This is also interpreted as the drug has passed through the membrane and is depleted from the membrane with a loss of drug a lower ionic conductivity.

| Drug | Mol. Wt. (Da) | % Throughput by DEA W/ Field (V) | % Throughput Control W/O Field (V=0) | Wavelength (nm) UV peak for Analysis | End point Conductivity ($pScm^{-1}$) |
|---|---|---|---|---|---|
| **Nimesulide (solid)** | **308** | **22** | **2.4** | **290** | **3.7 x10$^6$** |
| **"JCC 76" (solid)** | | **48** | **0.0** | **250** | **24 x10$^6$** |
| **Insulin (liquid)** | **5808** | **72** | **3.2** | **270** | **26 x10$^6$** |
| **Diphenhydramine (liquid)** | **255** | **81** | **17** | **214** | **48 x10$^6$** |

***Table: 4*** *% Through-put and end point conductivity by UV and Dielectric Analysis, respectively.*

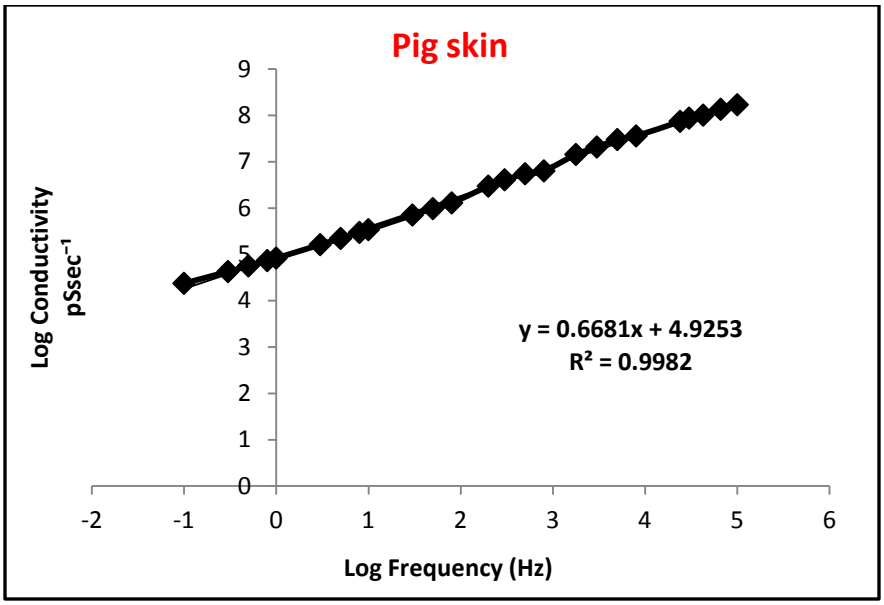


***Figure 27:*** *DEA of pig skin*

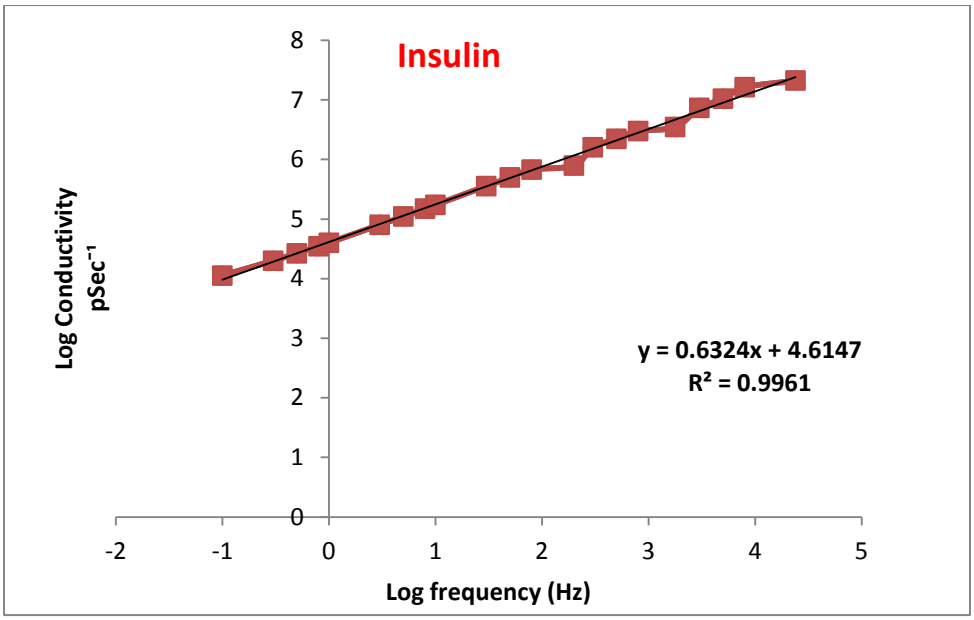


***Figure 28:*** *DEA of Insulin*

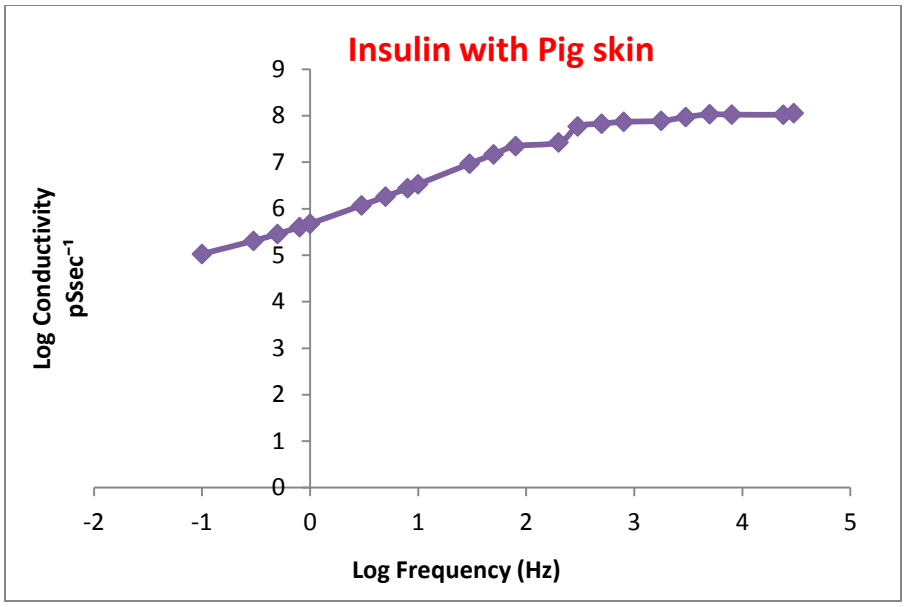


***Figure 29:*** *DEA of insulin behavior on pig skin*

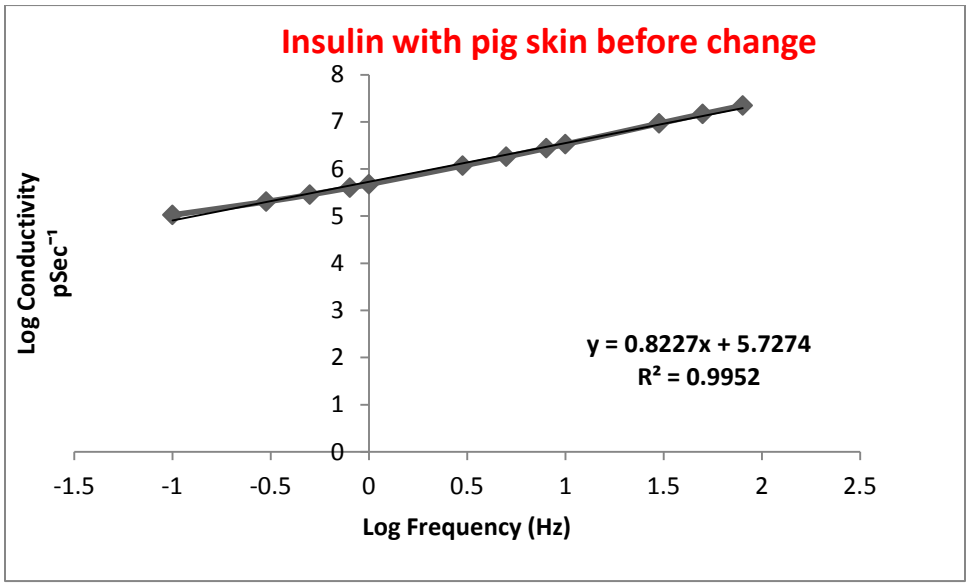


***Figure 30:*** *DEA of Insulin behavior on pig skin prior to the critical frequency of 100 Hz*

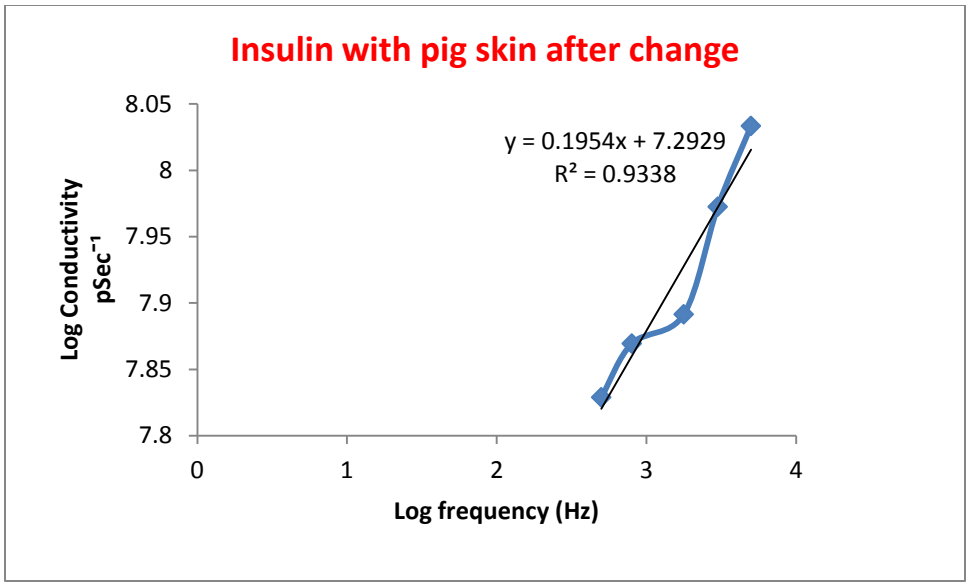


***Figure 31:*** *DEA of Insulin after the critical frequency of 100 Hz*

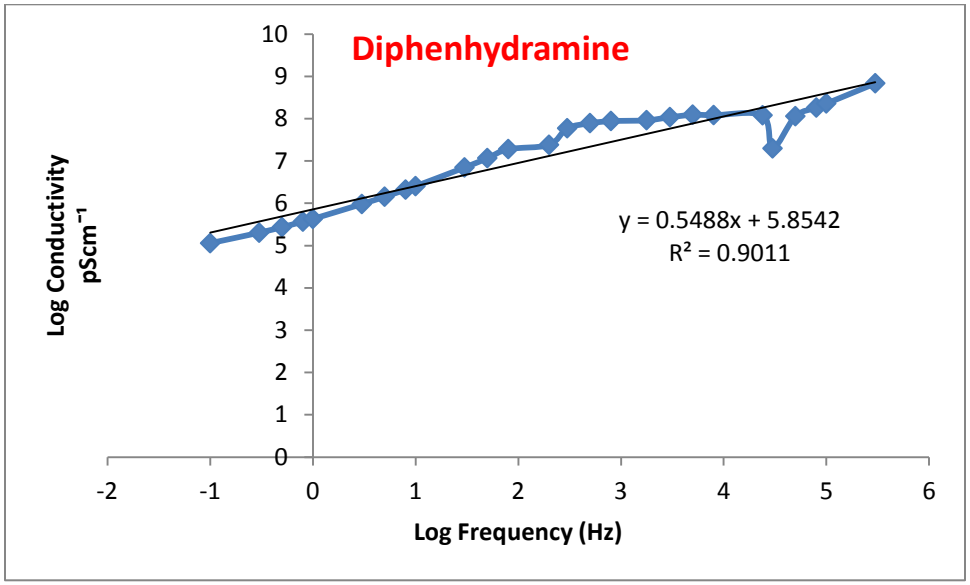


***Figure 32:*** *DEA of Diphenhydramine as a function of frequency*

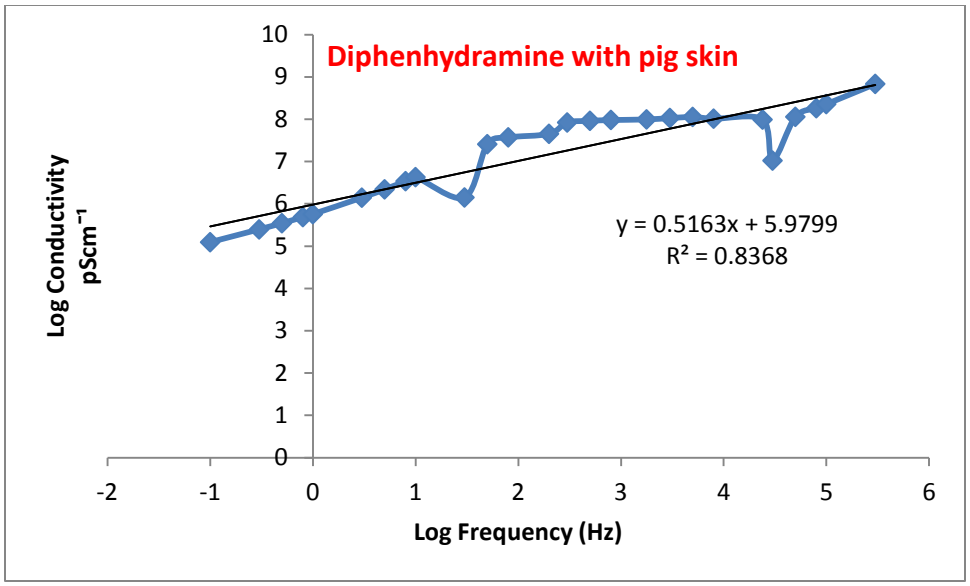


***Figure 33:*** *DEA of Diphenhydramine on pig skin*

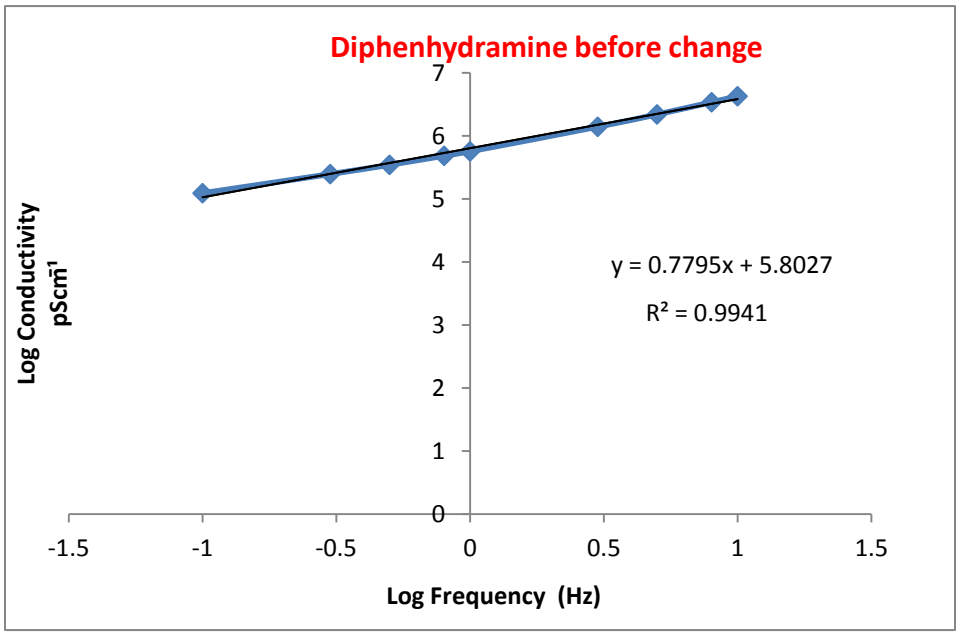


***Figure 34:*** *DEA of Diphenhydramine on pig skin prior to the 10 Hz critical frequency*

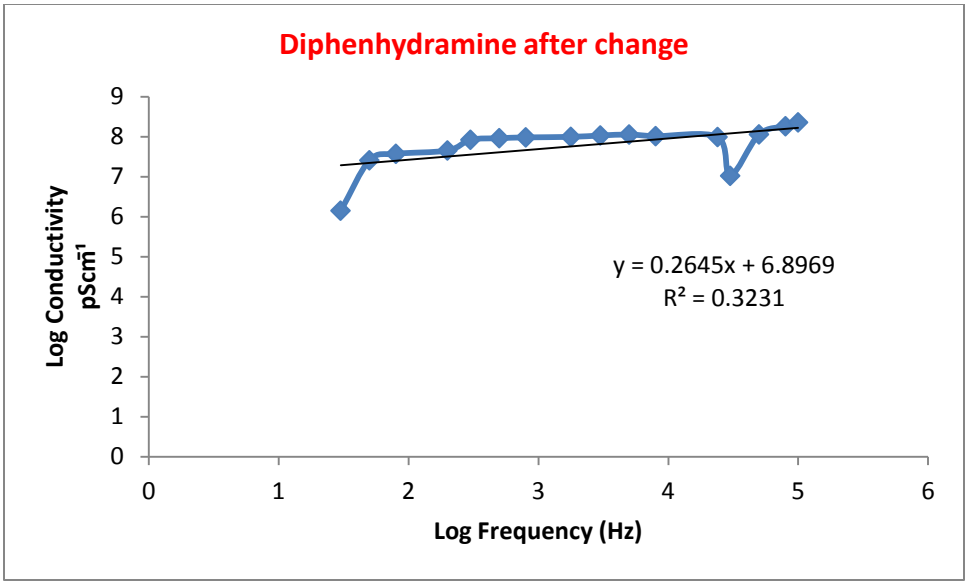


***Figure 35:*** *DEA of Diphenhydramine on pig skin after critical frequency*

*4.3.2 B-Cell Results*

4.3.2.1 Correlation Matrix

The correlation matrix of investigating variables and outcome measures showed strong relationships (|r|= 0.9 to 1.0) between Z, Z' and Z", indicating the strong consistency and validity of the measurements. A moderately positive relationship (r=0.4) is seen between Voltage and Z", based on the relationship between Z", which is proportional to conductivity, and current as defined by Ohm's law. Analysis also revealed a moderately negative (r = -0.49) relationship between pre- and post-test conductivity and low frequency.

| | *K* | *Time* | *Z'* | *Z''* | *Z* | *Voltage* | *High Freq.* | *Low Freq.* | *Pre-Test Z* | *Pre-Test K* | *Delta K* |
|---|---|---|---|---|---|---|---|---|---|---|---|
| K/pS cm-1 | 1.0 | | | | | | | | | | |
| Time/sec | -0.05 | 1.0 | | | | | | | | | |
| Z'/ohms | -0.30 | -0.05 | 1.0 | | | | | | | | |
| Z''/ohm | 0.27 | -0.01 | -0.94 | 1.0 | | | | | | | |
| Z/ohm | -0.30 | -0.04 | 1.00 | -0.96 | 1.0 | | | | | | |
| Voltage/V | -0.32 | -0.02 | -0.26 | 0.40 | -0.29 | 1.0 | | | | | |
| High Freq./Hz | -0.09 | 0.02 | -0.28 | 0.22 | -0.27 | 0.03 | 1.0 | | | | |
| Low Freq./Hz | -0.08 | 0.03 | -0.17 | 0.24 | -0.19 | 0.03 | -0.03 | 1.0 | | | |
| Pre-test Z/ohm | 0.18 | -0.15 | 0.29 | -0.30 | 0.29 | N/A | -0.08 | -0.61 | 1.0 | | |
| Pre-test K/pS cm-1 | -0.18 | 0.17 | -0.29 | 0.30 | -0.29 | N/A | 0.09 | 0.63 | -1.00 | 1.0 | |
| Delta K pS cm-1 | 0.78 | -0.19 | -0.18 | 0.17 | -0.18 | N/A | -0.16 | -0.49 | 0.76 | -0.76 | 1.0 |

***Table 5:*** *Correlation matrix results*

4.3.2.2 Factor Analysis

A factor analysis of the investigating variables and one outcome measure (K) found two significant factors (p-value=0.79). The first factor contains the conductivity and voltage variables and the second factor contains the time variable. The first factor explains 22 percent of the variance in the outcome measures and the second factor explains 20 percent of the variance, for a total of 42 percent of variance explained by the two factors. This indicates that although the study has captured some of the major driving factors of drug transport, other unique variables also contribute to variations in outcomes.

**Factor Loadings**

| | *Factor 1* | *Factor 2* |
|---|---|---|
| K/pS cm-1 | 0.997 | |
| Time/sec | | 0.996 |
| Voltage/V | -0.320 | |
| High Freq./Hz | | |
| Low Freq./Hz | | |

***Table 6:*** *Factor analysis*

## 4.4 Analysis Results

Increase in conductivity was identified in five of the 54 studies; implying drug transport is enhanced by the investigating variables in this study. The common features of the five sets of optimal parameters were a voltage of 1V and a low frequency of 0.1Hz.( figure 36, 37) Time was not found to be a significant factor in transport, indicating the process is not one of diffusion but is defined by the properties of the applied electric fields. Drug permeation appears to be driven by voltage and low frequency, in combination with an appropriate range of high frequencies.

***Figure 36:*** *Conductivity vs. Voltage* ***Figure 37:*** *Conductivity change vs. Frequency*

## 4.5 UV Analysis

Drug throughput into a saline solution below the pig skin membrane was measured using a UV-Vis concentration analysis technique in which study sample absorbances were fit to a linear calibration curve of standard samples. Peak absorbance was measured at 271.9nm and three aliquots were scanned three times each for a total of nine scans for each sample. Throughput ranged from 12 percent to 100 percent, with a

mean of 57 percent based on a constant dose of 1mL (100*uL*) Insulin, with each unit of Insulin equal to approximately 0.034mg for a total of 34mg in 1mL. Transport by weight ranged from 4mg (12 percent of 100*uL*) to 34mg (100 percent of 100*uL*). Membrane thickness ranged from 0.7mm to 1.8mm with a mean of 1.3mm and has a weak negative correlation (r=-0.3) with throughput. The average standard deviation for the UV-Vis scans was 0.016 and the average relative percent error of the absorbance readings was 1.8, with a range from 0.2 to 5.2.

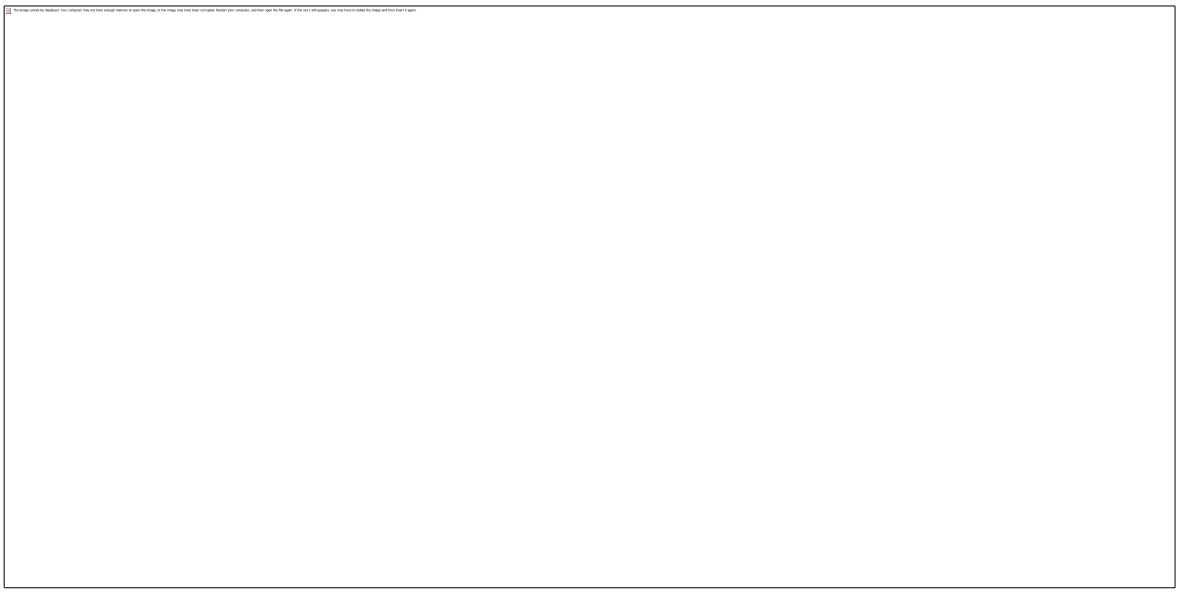

***Figure 38:*** *Average distribution of Insulin frequency Vs. % through put*

### 4.6 Conclusions

These results show the proposed series of successive AC fields was capable of transporting clinically significant amounts up to 100*uL* of the macromolecular drug Insulin (5,808 daltons) across membranes up to 1.8mm thick in as little as 400 seconds given an appropriate range of high and low frequencies coupled with an AC voltage signal of 1 to 4 Volts. Distance to cross the membrane was the most significant factor in

determining throughput. Analysis of pre- and post-test conductivity pointed to five sets of parameters with high conductivity change, which may be taken as an indication of drug penetration into the membrane separate from drug transported through the membrane to the solution below. In fact, the five studies with high conductivity changes had relatively low throughput values, including the lowest value recorded of 12 percent throughput. No localized heating or visible damage to membranes was observed.

## References


1. R.B. Shah, F. Ahsan, M.A. Khan, Oral delivery of proteins: progress and prognostication, Crit. Rev. Ther. Drug Carr. Syst. 19 (2005) 135–169.
2. A.Banga, Electrically Assisted Trasdermal and Topical Drug Delivery
3. R.I. Mahato, A.S. Narang, L. Thoma, D.D. Miller, Emerging trends in oral delivery of peptide and proteins, Crit. Rev. Ther. Drug Carr. Syst. 20 (2003) 153–214.
4. V. F. Lvovich, E. Matthews, A. T. Riga, L.Kaza, AC electrokinetic platform for iontophoretic transdermal drug delivery, *Journal of Controlled Release 145 (2010) 134-140.*
5. Current Status and Future Prospects in Transdermal Drug Delivery.
6. T. Shibajia, Y. Yasuharab, N. Odac, M. Umino, A mechanism of the high frequency AC iontophoresis, *Journal of Controlled Release 73 (2001) 37–47*.
7. Jia-You Fang, K.C. Sung, Hung-Hong Lin, Chia-Lang Fang, Transdermal iontophoretic delivery of enoxacin from various liposome-encapsulated formulations, *Journal of Controlled Release 60 (1999) 1–10.*
8. A.Jadoul, J.Bouwstra, V.Pre´at, Effects of iontophoresis and electroporation on the stratum Corneum Review of the biophysical studies, *Advanced Drug Delivery Reviews 35 (1999) 89–105.*
9. J. Varshosaz, Insulin Delivery Systems for Controlling Diabetes, *Recent Patents on Endocrine, Metabolic & Immune Drug Discovery 2007, 1, 25-40.*
10. A.Denet, R. Vanbever, V. Pre´at, Skin electroporation for transdermal and topical delivery, *Advanced Drug Delivery Reviews 56 (2004) 659– 674*.

11. R.H. Guy, Current status and future prospects of transdermal drug delivery, Pharm. Res. 13 (1996) 1765– 1768.
12. A.Jadoul, J. Mesens, W. Caers, F.Beukelaar, R.Crabbe, V.Pre´at, Transdermal Permeation of Alniditan by Iontophoresis: In Vitro Optimization and Human Pharmacokinetic Data, *Pharmaceutical Research, Vol. 13, No. 9, 1996*.
13. R. Langer, Transdermal drug delivery: past progress, current status, and future prospects, *Advanced Drug Delivery Reviews 56 (2004) 557– 558.*
14. A. Jadoul, J. Doucet, D. Durand, V.Pre´at, Modifications induced on stratum corneum structure after in vitri iontophoresis: ATR-FTIR and X-ray scattering studies, *Journal of Controlled Release 42 (1996) 165-173.*
*15.* G. Gwinup, A.N. Elias, N.D. Vaziri, A case for oral insulin therapy in the prevention of diabetic micro- and macroangiopathy, Int. J. Artif. Organs 13 (1990) 393–395.
*16.* E. Khafagy, M. Morishita , Y.Onuki, K. Takayama, Current challenges in non-invasive insulin delivery systems: A comparative review, *Advanced Drug Delivery Reviews 59 (2007) 1521–1546*
*17.* N. Kanikkannan, J. Singh, P. Ramarao, Transdermal iontophoretic delivery of bovine insulin and monomeric human insulin analogue, *Journal of Controlled Release 59 (1999) 99–105.*
*18.* M. J. Pikal, The role of electroosmotic flow in transdermal iontophoresis, *Advanced Drug Delivery Reviews 46 (2001) 281–305*.
19. N. Kanikkannan, Iontophoresis-Based Transdermal Delivery Systems, *Drug Delivery Biodrugs 2002; 16 (5): 339-347.*

20. R.I. Mahato, A.S. Narang, L. Thoma, D.D. Miller, Emerging trends in oral delivery of peptide and proteins, Crit. Rev. Ther. Drug Carr. Syst. 20 (2003) 153–214.

*21.* F.P. Kennedy, Recent developments in insulin delivery techniques: current status and future potential, Drugs 42 (1991) 213–227.

*22.* O. Ishikawa, Y.Kato, H. Onishi, T. Nagai, Y.Machida, Enhancement of transdermal absorption by switching iontophoresis, *International Journal of Pharmaceutics 249 (2002) 81_ 88.*

*23.* V.Lvovich, S. Srikanthan, R. L. Silverstein, A novel broadband impedance method for detection of cell-derived microparticles, *Biosensors and Bioelectronics 26 (2010) 444–451*

# CHAPTER V

# THERMAL ANALYSIS OF WATER AND MAGNESIUM HYDROXIDE CONTENT IN COMMERCIAL PHARMACEUTICAL SUSPENSIONS OF MILK OF MAGNESIA


## Abstract

A standard protocol was developed to determine the water content by thermal analysis of Milk of Magnesia (MoM). Differential Scanning Calorimetry (DSC) and Thermalgravimetry (TG) were used in a novel manner for examining the physical characteristics of the commercial pharmaceutical suspensions. Moisture analyzer and oven-dry methods validates the proposed protocol.

MoM consists primarily of water and magnesium hydroxide ($Mg(OH)_2$). Experimental design of the thermal analysis parameters were considered including sample size, flowing atmosphere, sample pan and heating rate for both DSC and TG. The results established the optimum conditions for minimizing heat and mass transfer effect. Sample sizes used were: (5-15 mg) for DSC and (30-50 mg) for TG. DSC analysis used crimped crucibles with a pinhole, which allowed maximum resolution and gave well

defined mass (water) loss. TG analysis used a heating rate of $10^{o}Cmin^{-1}$ in an atmosphere of nitrogen.

The heat of crystallization, heat of fusion and heat of vaporization of unbound water are 334, 334 and 2257 $Jg^{-1}$, respectively (3). The DSC average water content of (MoM) was 80%w for name brand and 89.5%w for generic brand, based on the relative crystallization, melting and vaporization heats ($Jg^{-1}$) of distilled water to recently purchased (2011) MoM samples. The TG showed a two step process, loosing water at 80-135$^{o}$C for unbound water and bound water ($MgO.H_2O$) at 376-404$^{o}$C, yielding a total average water loss of 91.9% for name brand and 90.7% for generic brand by mass. The difference between the high temperature TG and the lower temperature DSC can be attributed for the decomposition of magnesium hydroxide or $MgO.H_2O$. Therefore in performing this new approach to water analysis heating to a high temperature decomposed the magnesium hydroxide residue. It is our considered opinion that the DSC method is more accurate than the TG protocol for unbound water.

**Key Words:** Milk of Magnesia (MoM), Differential Scanning Calorimetry (DSC), Thermal Gravimerty (TG), Unbound water and Bound water

## 5.1 Introduction

In general, water can be organized by phases of matter: liquid, solid and gas. The liquid phase is the most common among all the water phases on the surface of the earth and this phase is noted as "water". The solid phase of water is a physically hard structure, which is commonly known as ice. The gas phase of water is recognized as vapor or the "vapor phase" of water. The physical chemistry of water is denoted as one molecule of water where two hydrogen atoms are covalently bonded to a single oxygen atom (2). Liquid water has no taste or odor and at normal atmospheric temperature and pressure water is colorless, however it can have a very light blue hue. Ice is colorless, water vapor or steam cannot be seen as a gas. At standard conditions, 25˚C and pressure 1atm water is a liquid. The water molecule has a net positive charge on the hydrogen atoms and a net negative charge on the oxygen atom. The net result is that each water molecule has a dipole moment. Water is a polar liquid that can form a hydronium ion ($H_3O^+$) and is interactive with hydroxide ion ($OH^-$).

$$2\ H_2O\ (l) \rightleftharpoons H_3O^+\ (aq) + OH^-\ (aq)$$

The heat of vaporization, ($\Delta H_v$), is the energy to change a given quantity of water into its gas phase at the standard temperature and pressure. Heat of vaporization for water is 2257 $Jg^{-1}$. The heat of fusion ($\Delta H_f$) is the result of the change in the phase of water from solid to liquid which occurs at the melting temperature ($T_{m)}$). Heat of fusion for water is 334 $Jg^{-1}$. The heat of crystallization ($\Delta H_c$) is the result of the change in the phase of water from liquid to a solid which occurs at the crystallization temperature ($T_{c)}$). Heat of crystallization for water is 334 $Jg^{-1}$[3].

The following is a summary from W.J. Sichina paper "Characterization of Water of Hydration of Pharmaceuticals Using the DSC". He developed a test to characterize the properties associated with the waters in a pharmaceutical material. The method includes automated sample pan puncturing accessory for the study of free and bound waters in pharmaceuticals. An additional protocol for determining hydrated pharmaceuticals materials is DSC. Sichina's DSC protocol includes a thermal program: heat from room temperature at $10^{\circ}Cmin^{-1}$, sample mass approximately 4 mg, sample pan 30 µl aluminum pan with a hole, and purge gas nitrogen [2].

Milk of Magnesia is a suspension of magnesium hydroxide $Mg(OH)_2$ in water**.** It is widely used as an antacid to neutralize stomach acid and laxatives. Low solubility of $Mg(OH)_2$ in water makes it a weak base and considered as a strong electrolyte. The United States Pharmacopeia states that single strength Milk of Magnesia should contain not less than 90.0 % and not more than 115.0% of the labeled amount of 80 mg of $Mg(OH)_2 mL^{-1}$. It is commercially produced by the precipitation of magnesium hydroxide paste from seawater. The paste can have varying degrees of viscosity, which determines whether a suspending agent is required or not. Water, whose melting /crystallization temperature and enthalpy are not significantly different from those of normal (bulk) water, is called free water or freezing water or unbound water. Those water species exhibiting large differences in transition enthalpies and temperatures, or those for which no phase transition can be observed calorimetrically are referred to as bound water.

The purpose of these experiments is to find the best analytical method to determine bound, unbound water and water activity. Oven-dry and moisture analyzer

methods are traditional methods, which are used in this experiment as controls. They are used to determine the total water lost from the test samples. Since both traditional methods can only determine the total amount of water lost, these methods cannot be used to determine bound, unbound water and water activity.

TG rapidly measures changes in mass as a sample is heated and is eventually vaporized. This can be used to create a water loss profile that can show the different temperature ranges in which water and other components of a sample vaporize. DSC analyzes the phase changes in matter and can also be used to determine a water loss profile. Both methods can be used to determine the amounts of bound and unbound water and from which can be used to determine the total amount of water lost in a sample. This will be compared to the traditional controls to determine if the novel methods can be accurately used to determine bound, unbound, and total water in a sample of milk of magnesia.

## 5.2 Experimental Methods

The laxatives used in the study were a brand name milk of magnesia and a generic brand milk of magnesia. Each product was tested for water content using two conventional methods: 110°C oven, and moisture analyzer and two novel methods: Differential Scanning Calorimetry and Thermalgravimetry.

### *5.2.1 110°C Oven Method*

This method used small aluminum pans, a vacuum oven set to 110°C, and a desiccator. First, the aluminum pans were analytically weighed and recorded to 3 decimal places. Next, two samples of each product were analytically weighed from 1.5-2.0 grams onto

separate pre-weighed pans to 3 decimal places and recorded. Then the pans were placed into the vacuum oven. The oven used was a Fisher Scientific Isotemp® vacuum oven model 282A (figure 39). Pans and samples were left in the oven for 3 hours at 15 kPa vacuum. After 3 hours, the pans were removed from the oven and immediately placed into desiccator under vacuum for 1 hour. After one hour, the pans were removed from the desiccators and were analytically weighed and recorded to 3 decimal places.

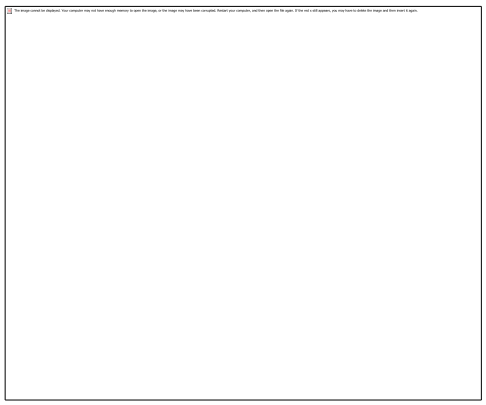

***Figure 39:*** *Fisher Scientific Isotemp® 282A*

*5.2.2 Moisture Analyzer Method*

Samples of each product were analyzed for moisture content using the Lab wave 9000 Moisture Analyzer (figure 40). The moisture analyzer uses an analytical balance inside of a microwave oven (figure 41), which dries the sample, while recording a change in mass. At the end of the test the percent moisture of the sample is automatically calculated. First, two absorbent pads are placed on the analytical balance inside the moisture analyzer and the balance is tared. Next, 1.0-1.5 grams of sample is placed in between the absorbent pads. Then the moisture analyzer is activated, using 80% power. The sequence is completed when the moisture analyzer no longer records a change in mass. The

instrument then displays the percent moisture, percent solids, and the amount of time it took to complete the analysis.

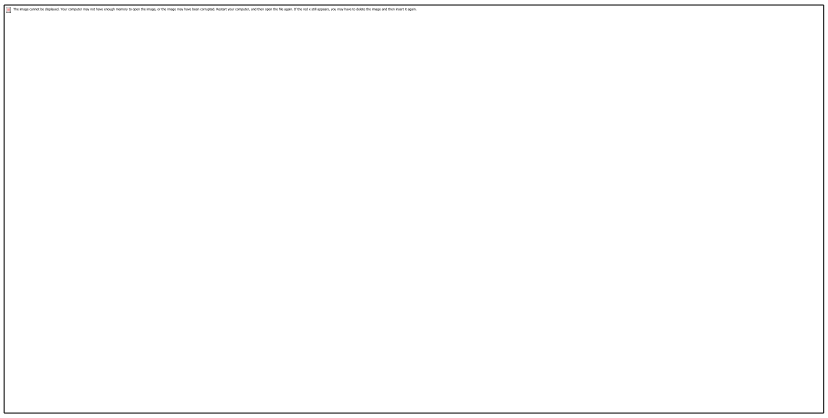

***Figure 40:*** *Lab wave 9000* ***Figure 41:*** *Inside*

*5.2.3 Thermogravimetry Method (TG)*

A TA Instruments Hi-Res Thermalgravimetric Analyzer Model 2950 (figure 42) was used to measure bound and unbound water in milk of magnesia samples. The samples were prepared by placing one drop of material on to a pre-tared platinum TG pan. The pan was placed onto the auto-loading mechanism of the TG analyzer and an automated loading sequence was initiated. The sample is placed into a furnace which heats the sample, while measuring the mass of the sample every 0.5 second. The TG experimental conditions were: Ramp 10°C per minute to 500°C in nitrogen. 30-50 mg of sample was used in each run.

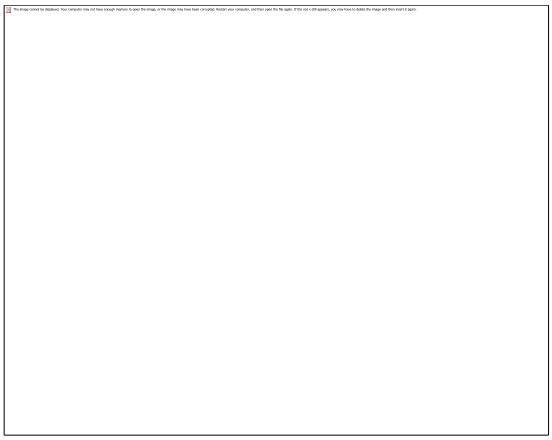

***Figure 42:*** *Thermalgravimetric Analyzer Model 2950*

*5.2.4 Differential Scanning Calorimetry Method (DSC)*

The Mettler DSC $823^e$ 20 instrument (figure 43) was used to measure the heat flow properties of the milk of magnesia samples which involve exothermic or endothermic processes as a function of time and temperature. Samples were placed in solid fat index (SFI) aluminum pans with sampling size ranging from 5 mg to 15 mg, covered with a lid and were sealed. The samples were cooled from 25 to -50°C and then heated to 120°C at $5^{\circ}Cmin^{-1}$ heating rate with nitrogen gas purge of 50 $mL.min^{-1}$. Closed pans were used in this study. The DSC scan provided data of the following thermal properties: Heat of fusion ($\Delta H_f$), melting temperature ($T_m$), peak melt temperature ($T_{mp}$), heat of crystallization ($\Delta H_c$), crystallization temperature ($T_c$), peak crystallization temperature ($T_{cp}$), heat of vaporization($\Delta H_v$), vaporization temperature($T_v$) and peak vaporization temperature($T_{vp}$).

***Figure 43:*** *Mettler Toledo DSC*

### 5.3 Results and Discussion

The results of % water from the 110°C pan method are shown in table 7:

| **Source drug suspension** | Sample | Water | Average | SDEV |
|---|---|---|---|---|
| Milk of Magnesia (Name Brand) | 1 | 91.8% | 91.8% | 0.0 |
| | 2 | 91.7% | | |
| Milk of Magnesia (Generic Brand) | 1 | 90.6% | 90.%6 | 0.1 |
| | 2 | 90.7% | | |

***Table 7:*** *Results of % water from pan method*

The results were obtained by subtracting the mass of the pan and sample after testing, from the initial mass of the pan. The difference was the amount of solids left in the pan. From there, the mass of the material left in the pan was subtracted from the initial mass of the sample. The data shows that the amount of water in the commercial brand of milk of magnesia to be 91.8% and the generic brand of milk of magnesia was 90.6%. The

moisture analyzer results were virtually identical to the results obtained from the 110° C pan method as seen in Table 8.

| | Total Water (Oven)* | Total Water* (Analyzer) |
|---|---|---|
| MoM (Name Brand) | 91.8% | 91.9% |
| MoM (Generic Brand) | 90.6% | 90.8% |

**Average values*

***Table 8:*** *Comparison of two conventional methods for water content in milk of magnesia*

TG data was analyzed using *Universal Analysis 2000,* by TA Instruments, version 4.4A. The data was plotted and analyzed using the first derivative of the percent (%) mass loss versus temperature in °C. From there, each peak was identified and the percent material loss was calculated. Also identified were the initial and end points at which mass loss began and ended. All remaining material in the sample was calculated as percent residue. The results are shown in figures 44 and 45.

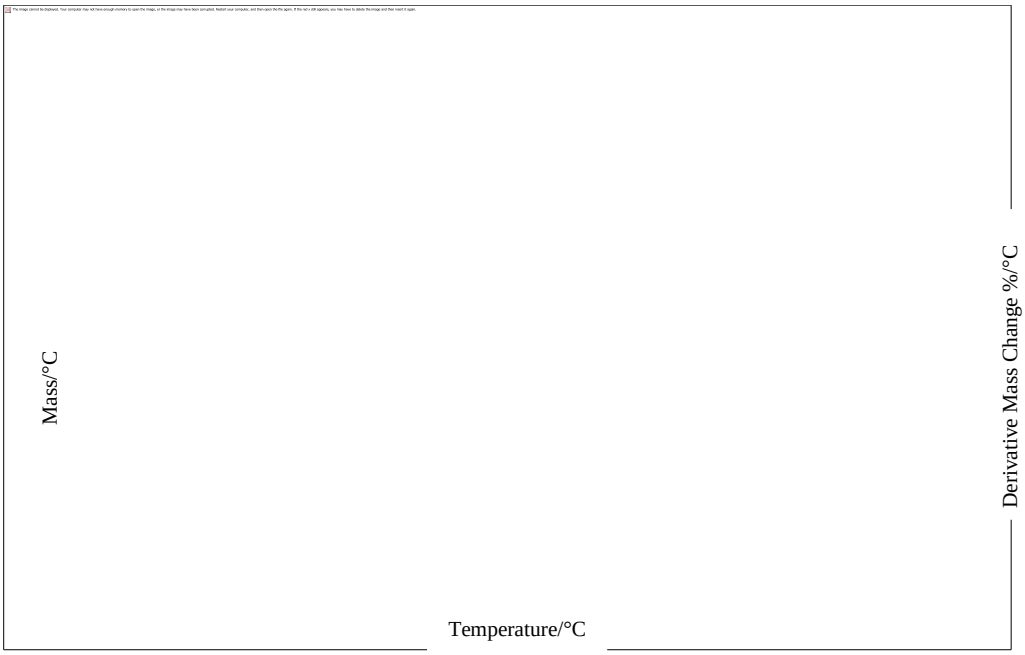


***Figure 44** : TG analysis for name brand*

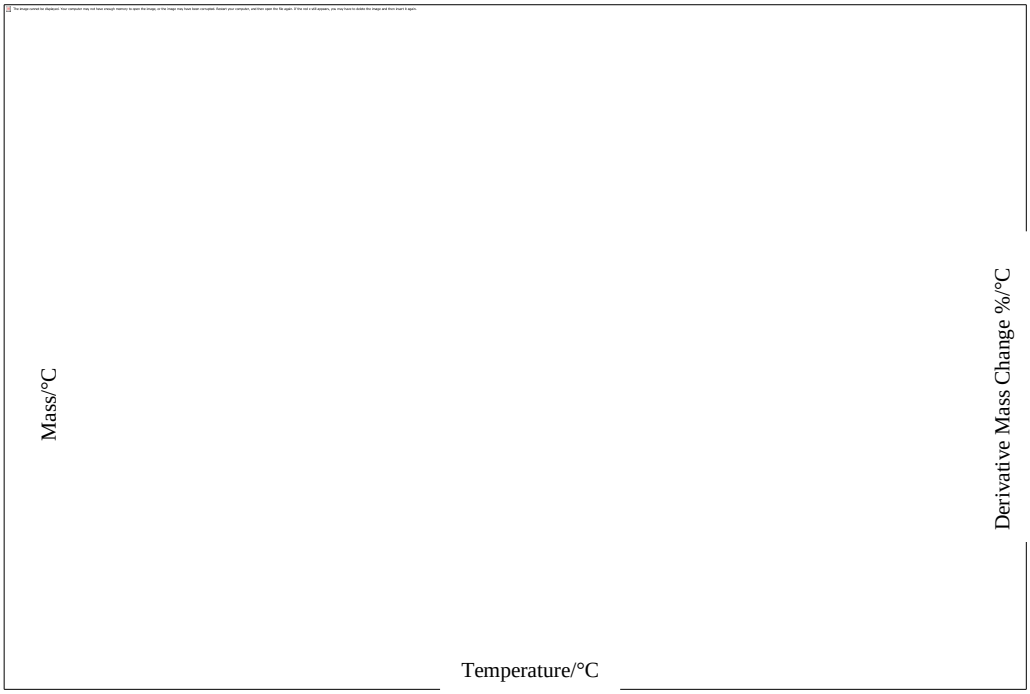


***Figure 45:** TG analysis for generic brand*

In comparison to the conventional methods, TG analysis showed both bound and unbound water. Water vaporization results are shown in table 9. The unbound water vaporized between 80°C and 119°C in the name brand MoM. The unbound water in generic brand MoM vaporized between 91° and 135°C. The bound water in the name brand MoM vaporized between 376° and 398°C and between 374° and 404°C in the generic brand MoM.

| | Unbound Water | Bound Water | Total Water |
|---|---|---|---|
| MoM (Name Brand) | 88.0% | 2.2% | 90.2% |
| MoM (Generic Brand) | 88.3% | 2.4% | 90.7% |

***Table 9:*** *% of unbound water and bound water for test samples by TG*

DSC results are summarized in the Figures 46, 47 and 48 as well as tables 10 and 11. The free water concentrations were determined based on the cool and heat DSC curves. The heat of crystallization, $\Delta H_c$ (from the cooling curve) and the heat of fusion, $\Delta H_f$ (heating curve after crystallization) were calculated for pure water and the commercial suspensions of milk of magnesia produced by a name brand and a generic pharmaceutical contract packager. The free or unbound water are the focus of this study and by difference the amount of water relative to the "pure" water. Assuming a two component suspension of water and magnesium hydroxide ($Mg(OH)_2$ suspended in the water), various samplings of the commercial suspensions were evaluated by the DSC curves. The average, standard deviation and percent relative error were calculated from the $\Delta H_c$ and $\Delta H_f$ measured and are reported in table 10. The standard deviation was ± 17 to ± 22 and the % relative error was 5.3 to 7.6% for the heat measurements. The heat of

vaporization was recorded during the DSC run but due to baseline variations and sampling techniques were not used for the calculation of the water content.

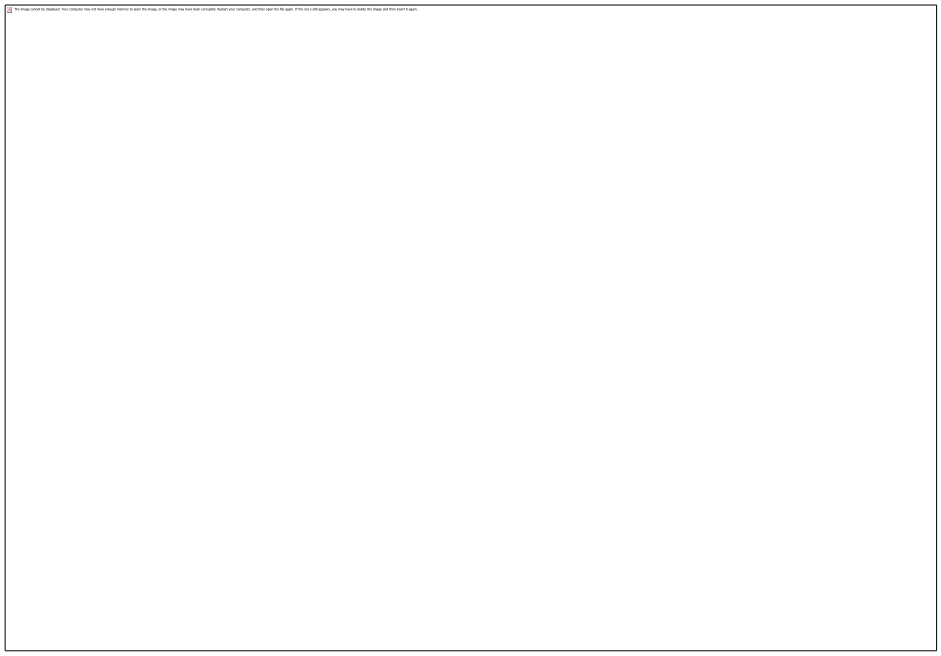

***Figure 46:*** *DSC analysis for distilled water*

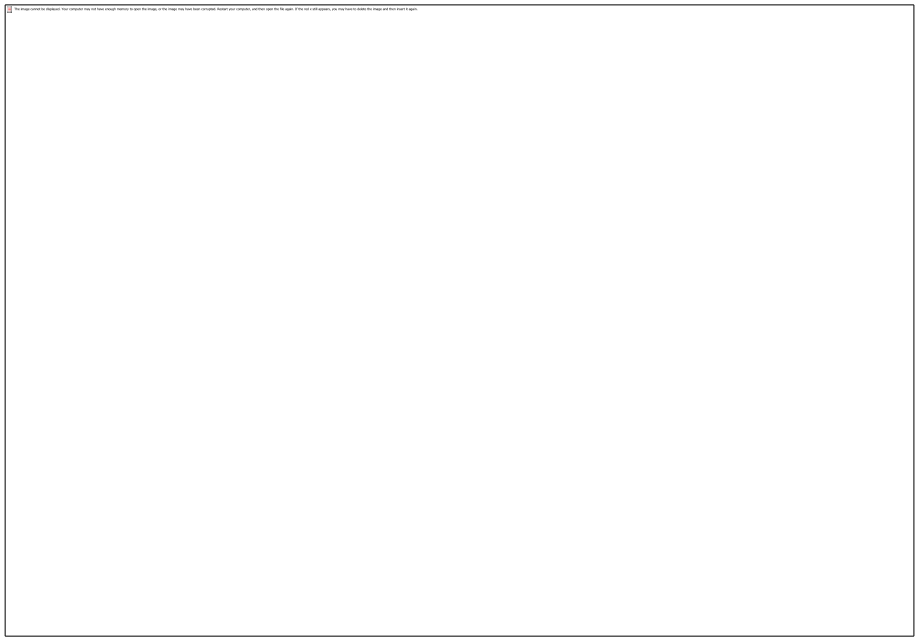

***Figure 47:*** *DSC analysis for name brand MoM*

***Figure 48:*** *DSC Analysis of Generic brand*

| Drug (liquid) | Average $\Delta H_c/Jg^{-1}$ | Standard deviation/± | % Relative error | Average $\Delta H_f/Jg^{-1}$ | Standard deviation/± | % Relative error |
|---|---|---|---|---|---|---|
| Distilled water | 338 | 19 | 5.5 | 373 | 20 | 5.3 |
| Milk of Magnesia (Name Brand) | 276 | 17 | 6.1 | 291 | 18 | 6.2 |
| Milk of Magnesia (Generic Brand) | 312 | 18 | 5.4 | 326 | 22 | 7.6 |

**All values $H_c$ and $H_f$ are based on three samplings*

***Table 10:*** *Average, standard deviation and % relative error of $\Delta H_c$ and $\Delta H_f$*

| Drug (liquid) | $T_c$ °C | $T_{cp}$ °C | $\Delta H_c$ $Jg^{-1}$ | Relative $\Delta H_c$% | $T_m$ °C | $T_{mp}$ °C | $\Delta H_f$ $Jg^{-1}$ | Relative $\Delta H_f$% | Average of ΔHc and ΔHf |
|---|---|---|---|---|---|---|---|---|---|
| Distilled water | -18 | -14 | 338 | 100 | 0 | 3.0 | 373 | 100 | 100 |
| Milk of Magnesia (Name Brand) | -17 | -13 | 276 | 82 | -1.2 | 2.0 | 291 | 78 | 80 |
| Milk of Magnesia (Generic Brand) | -17 | -12 | 312 | 92 | -1.3 | 2.0 | 326 | 87 | 89.5 |

***Table 11****: Relative $\Delta H_c$, $\Delta H_f$ and average of $\Delta H_c$ and $\Delta H_f$*

The final summary of the DSC analysis includes: the temperature profile of the free or unbound water, its water content relative to the $\Delta H_f$ and $\Delta H_c$ and the average result of the water by both analytical techniques, see table 12. The Milk of Magnesia, name brand and generic brand was 80.0% and 89.5%, respectively by DSC. Therefore, there appears to be a 10% variation between the two MoM commercial samples.

| Source Suspension | Oven 110˚C | Moisture Analyzer | TG | Mettler DSC | Viscocity* mPa·s |
|---|---|---|---|---|---|
| Milk of magnesia (Name brand) | 91.8% | 91.9% | 90.2% | 80.0% | 1585 |
| Milk of Magnesia(Generic Brand) | 90.6% | 90.8% | 90.7% | 89.% | 2980 |

**Brookfield DV II+ Viscometer (#3 RVT spindle at 20rpm)*

***Table 12****: Percent of water content from all the techniques and viscosity for test samples*

An overview of the water content by four analytical techniques is reported in table 12. The water content for the Oven Test at 110˚C, the Moisture analyzer, TG and DSC for:

Name Brand was 91.8, 91.9, 90.2 and 80.0%w, respectively.

Generic Brand was of 90.6. 90.8, 90.7 and 89.5%w, respectively

The differences between the brand and generic were the same for the oven, moisture analyzer and TG methods. There was a repeatable difference based on the DSC analysis of 10% more water in the generic sample. Further, there was a sizable viscosity difference of 88% between the brand and generic. The generic had more water and a higher viscosity. The latter may be due to the additional additives denoted by 20 mg calcium and 2 mg sodium in the generic product. The calculation of water activity was developed to account for the intensity with which water associates with various non-aqueous constituents, e.g. MOM. It is a measure of the energy status of the water in a system (10, 11, and 12). It is defined as the vapor pressure of a liquid divided by that of pure water at the same temperature, yielding a value of one or 100%. It is our interpretation that the difference noted in the DSC analysis is due to water activity and can be uniquely evaluated by DSC.

**5.4 Conclusions**

The conventional methods of water analysis, oven and moisture analyzer provided total water. TG is used to determine the bound and unbound water in MoM. DSC uniquely discovered 10% more water in the generic probably due to water activity. The differences in alkali metal content can be associated with the DSC water activity or may be related to the enhanced viscosity of the generic brand.

## References


1. Peter J. Haines, Principles of thermal analysis and Calorimetry.
2. R.C. Mackenzie, 'Nomenclature in Thermal Analysis, Part IV', Thermochimica Acta, 1979, 28, 1-6
3. http://en.wikipedia.org/wiki/Properties_of_water
4. J.G. Dunn, Encyclopedia of Analytical Chemistry, 2000, 15, 13206-13226.
5. Y. Laureiro, A. Jerez, C. Pico, and M.L. Veiga, Thermochimica acta, 1991, 182, 47-56
6. Chen, S. Hwang, and S. Chen, Industrial Engineering and Chemistry Research, 1989, 28, 738-742
7. B.V. L'vov, A.V.Novichikin, and A.O.Dyakov, Thermochimica acta, 1998, 315, 135-143
8. H. Hatakeyama, T.Hatakeyama, Thermochimica acta, 1998, 308, 3-22
9. T. Hatakeyama, K. Nakamura, H.Hatakeyama, Thermochimica acta, 1988, 123, 153-161
10. K.D.Ross, Journal of Food Science, 1978, 43, 1812
11. Fennema, O.R., Ed. (1985). Food Chemistry - Second Edition, Revised and Expanded. New York: Marcell Dekker, Inc. pp. 46-50.
12. Bell, L.N., and Labuza, T.P. 2000. Practical Aspects of Moisture Sorption Isotherm Measurement and Use. 2nd Edition AACC Egan Press, Egan, MN

# CHAPTER VI

# AC ELECTROKINETIC PLATFORM FOR IONTOPHORETIC TRANSDERMAL DRUG DELIVERY


## Abstract

Iontophoretic and electroporation transdermal delivery modes of ionic drugs have been utilized in a number of clinical and biomedical devices. However, applications of these methods have been found challenging for the delivery of many non polar and high molecular weight clinically important drugs. The main goal of the present study is to investigate whether transdermal transport of non polar macromolecular drugs such as insulin and terbinafine can be safely enhanced as a result of their polarization and activation by AC electrokinetic forces. An in vitro delivery system was developed to simulate a clinical application, where transdermal non invasive delivery of medication through a biological membrane is motivated by a combination of AC electrokinetic and AC iontophoresis protocols generated on a device located external to the membrane. The developed method resulted in an average transdermal delivery of 57% of insulin and 39% of terbinafine during several minutes long delivery cycle, which is at least an order of magnitude improvement over the results reported for these drugs in the literature for

various passive and active transdermal delivery protocols. For the proposed drug delivery model quantification of the amounts of transported drugs and their relationship to experimental parameters, such as AC voltage amplitude and frequency, treatment time, and membrane thickness were investigated. Experimental results validated a computational model simulating the effects of major electrokinetic forces on drug particle in non uniform AC electric field. The presented transdermal approach overcomes many limitations of existing drug delivery technologies, providing efficient, regulated, localized, non invasive and safe delivery method for high molecular weight non polar macromolecules such as insulin.

**Key words**

Electrokinetics, Iontophoresis, Impedance, Insulin, Terbinafine, Transdermal

## 6.1 Introduction

Over the past decade non invasive transdermal drug delivery has become increasingly common. Transdermal drug delivery offers many benefits over oral, IV and injection therapies, in which procedures often result in adverse clinical side effects, and/or clinically sufficient quantities of the active ingredient do not reach the intended organ either fast enough or in high enough concentrations. That typically occurs because of the partial medication degradation when passing through various physiological environments (e.g. low pH values in the stomach), slow or incomplete absorption, or adverse affect on healthy organs and tissues. Transdermal procedures provide improved bioavailability and pharmokinetics, offering localized non invasive treatment, prolonged controlled release, and increased patient compliance. However, only a limited number of drug candidates have been successfully developed into suitable transdermal formulations because of the formidable dermal barriers such as stratum corneum outer layer of the skin. Further advancements in transdermal methods are required, especially for delivery of high molecular weight non ionic drugs [1]. Most of contemporary transdermal products are based on passive diffusion of a drug through skin over time. More recently, “active” iontophoresis drug delivery methods that may transfer a drug at a controlled rate have been developed and commercialized as transdermal patches [1-9]. Transdermal iontophoresis is a technology that enhances drug transport across the skin barrier with the assistance of an electric field. The mechanisms of transdermal iontophoresis include electrophoresis (EP) [10-12], electroosmosis (EO) [13, 14] and electroporation [15, 16]. Direct current (DC) iontophoresis is the most common type. Electroporation and

iontophoresis skin treatment have been shown to be effective through induced disorganization of lipid bylayers of stratum corneum and increase in skin hydration [5-7].

High current intensity (in case of electroporation) or extensive treatment times (in case of DC iontophoresis) can potentially lead to electrochemical burns, pain, and skin irritation [5, 6]. It has been suggested that AC iontophoresis can eliminate these negative side effects [17, 18]. Although high amplitude AC field applied in frequencies exceeding 10 Hz may provide less flux enhancement than DC field, significant flux enhancement has been observed during AC iontophoresis at constant current or constant voltage [17-21]. It has been shown that the AC electric field reduces skin electrical resistance by the mechanism of electroporation similar to that which occurs during DC. This electroporation effect has been found to dramatically increase with the AC voltage amplitude [20]. The flux enhancements due to EP and EO have been shown to be dependent on the AC voltage and AC frequency range [18].

Iontophoretic methods, however, were shown to be only of a very limited efficiency in transdermal transport of many clinically important non polar and high molecular weight drugs (such as insulin and terbinafine) [2]. Even for longer treatment times transdermal delivery of conventional insulin in humans has been largely unsuccessful presumably due to its weak ionization and partial polymerization, although a delivery of modified, strongly ionized monomeric form of insulin was successful in animals [22]. Inducing a temporary polarization on otherwise non polar macromolecules may result in better overall compliance with iontophoretic transdermal transport.

Recent years have witnessed significant advances in the field of electrokinetic manipulation of various biological species. Electrokinetic forces, such as EP EO, and

dielectrophoresis (DEP) have been widely used for manipulation, detection and separation of nano- and microparticles, such as proteins, bacteria, DNA, and blood cells [23-27]. Magnitude of forces can range widely, depending on particle size, position away from electrode and characteristic dimension of the electrode. A useful approach to manipulate particles at the microscale is to use electric fields to apply long range EP forces to charged particles, or induce dipoles and separate particles using a relatively short-range DEP. Electrokinetics has shown to be ideal for the manipulation of particles with sizes down to 20 nm, when small electrode channels (100 nm) and high voltages (~10 V) are utilized [24]. Electric fields work optimally with microscale particles and MEMS devices, integrating seamlessly with microfluidics and electrochemical sensors [27].

Relatively few systematic studies of AC motivated drug delivery methods in clinical settings, in particular those of higher molecular weight drugs, have been performed [28-30]. AC electrokinetics with its ability to vary effects of different forces on a particle may potentially become a highly effective method of drug delivery through biological membranes. However, the efficiency of drug delivery has to be optimized while making sure that currents through tissue membranes are kept low, treatment times are short, and the risk of localized electrical heating and other potential side effects are controlled. The main goal of this study was to investigate whether transdermal transport of two macromolecular drugs — insulin and terbinafine could be safely enhanced using the principles of AC electrokinetics.

## 6.2 Materials and methods

### *6.2.1 Materials*

Terbinafine hydrochloride (Lamisil) is a synthetic non polar antifungal drug with a molecular weight of 291.43 g/mol and molecular size of ~0.78 nm. For terbinafine delivery studies Lamisil cream formulation (1% terbinafine, or 10 g/L), widely available over the counter, was selected. Insulin is a high molecular weight (5808 Da or ~9500 g/mol) peptide hormone with the interior composed of non polar amino acid side chains, while the exterior contains polar amino acid side chains. The molecular dipole moment of a monomer insulin molecule is a fairly sizeable 72 D at 25 °C [31]. The molecule has a size of ~2.8 nm but larger aggregates may grow in time in aqueous solutions. For transdermal insulin delivery studies, Humalog® N (Eli Lilly, Indianapolis, IN) was chosen as a standard rapid acting insulin formulation in wide clinical use. Humalog® N is an isophane suspension of human insulin in a 10 mL vial of 1000 units, or approximately 4.17 g/L. Viscosity (0.001 Pa s), thermal conductivity (0.6 J/m sec K), permittivity (80) and electrical conductivity (10 μSm/m) of background mediawere taken to be approximately equal to those of water at roomtemperature. For insulin and terbinafine the values for permittivity (55 and 20, respectively) and conductivity (500 μSm/m and 100 μSm/m, respectively) were estimated from the impedance measurements, in agreement with the literature data on these drugs and their amino acid components [31]. Insulin and terbinafine conductivity values were confirmed by the measurements of the particle seizes and the zeta potentials (−20.1±1.3 mV and −6.6± 1 mV, respectively) at physiological pH 7.4 (Brookhaven Zeta PALS,Brookhaven Instruments, Holtsville, NY).

Excised pig skin and cow hoof were selected to serve as models of human skin and nail tissues, respectively [32, 33]. Animal tissues are readily obtainable in sufficient quantities to allow conducting properly controlled and reproducible multiple experiments. Pig skin samples with thickness ranging from 0.1 cm to 0.2 cm were obtained from the breast region of adult Yucatan pigs because of the lower density of hair follicles in this area, and were stored in sealed plastic bags in a refrigerator at −80 °C before use. The surfaces of the skins were cleansed with a mild skin-cleaning gel normally used for bioelectrical measurements and residual hair was removed with clippers. The epidermis and upper dermis were removed with a dermatome. 0.1 cm thick (±5%) cow hoofs were washed in the donor compartment buffer, dried, and stored in desiccator until use. The surface areas of both membranes were cut to approximately 2 cm×2 cm.

The membranes were mounted between two side-by-side diffusion chambers (diffusion surface area around 4 cm2 and cell volume of 4 mL) with the stratum corneum side facing the donor chamber. The biological membranes were sealed properly to avoid cross contamination of the “receiver” and the “donor” chambers. Approximately 500 μg samples of Lamisil cream or 500 μL of Humalog® solution were placed in the donor chamber. The receiver chamber was filled with phosphate buffered saline (PBS), containing 1.5% bovine serum albumin (BSA) (pH 7.4) or absorbent cloth was used to capture transported substance and overnight. The pH of the receiver solution was checked in a few occasions and was found to be essentially the same during the experiments. The receiver chamber was thermoregulated at 32±1 °C (skin temperature in vivo) in heated bath system (Lauda, Lauda-Königshofen, Germany). Both donor and receiver chamber solutions were replaced after each experiment. The experimental system composed of the

donor and the receiver chambers, the membranes, and the iontophoretic electrodes, were housed in a rectangular (2 cm×2 cm×2 cm) polyamide cube designed and manufactured in-house (Figure 49A). The system employed three separate voltage and current carrying electrodes — a counter electrode prepared out of a 0.1 cm thick stainless steel 316 metal film (Electrode 1), and two interdigitated iontophoretic electrodes (Electrode 2 and Electrode 3) placed directly on top of the stratum corneum layer of the membranes in the donor chamber. The counter Electrode 1 with a surface area of 4 cm2 was custom fit to the cell exactly and was separated from the "top electrode" plane by 300 μm thick TeflonR spacers. Electrodes 2 and 3 were machined out of stainless steel 316 into sets of interdigitated comb-shaped fingers with a thickness and height of 0.05 cm, and the length of 1.8 cm.

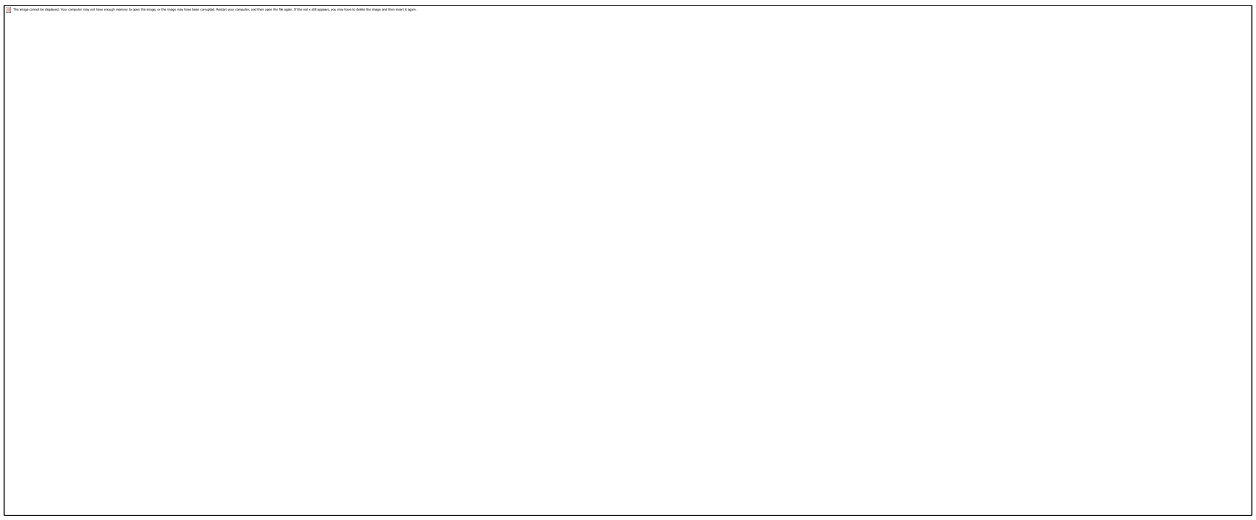

***Figure 49****: Cross-section (A) and top view with counter electrode removed (B) of the experimental set-up: 1 — counter Electrode 1; 2 — Teflon spacer; 3 — medication; 4 — comb-shaped Electrodes 2 and 3; 5 — air channels through Electrodes 2–3; 6 — biological tissue membrane; 7 — spring supports; 8 — B-Cell housing; 9 — electrical connectors to Electrodes 1–3; 10 — receiver solution or absorbent cloth; 11 — temperature probe.*

The gaps between the adjacent electrode fingers were fixed at 20 μm. Resistance of the electrode array in the background solution was measured at 22 k Ohm. The resulting plane composed of Electrodes 2 and 3 allows transport of compounds at the donor chamber in the direction perpendicular to the plane toward the stratum corneum interface, providing a realistic model of a transdermal drug delivery with the electrical field being applied on a medication located externally to the membrane. The cell was equipped with a temperature probe with an accuracy ±1 °C to monitor possible Joule heating effects.

*6.2.2 Experimental methods*

Impedance/Dielectric Analyzer (Novocontrol GmbH, Hundsangen Germany) using ZG4 cell adapter in a two-electrode arrangement was employed to supply the excitation signals to the electrodes; to determine the system impedance responses as a function of time, AC voltage and frequency; and to examine impedance changes in the membranes after the experiments. The impedance frequency scans were performed between 0.1 and 100,000 Hz with AC voltage amplitudes (peak-to-baseline) between 100 mV and 10 V and no DC offset. This analysis was used to evaluate impedance mismatches (Clausius–Mossotti polarization factor) between the media and the drug molecules as a function of applied AC frequencies [34]. In the developed drug delivery model, the intention was to subject the drugs to "polarization" AC electric perturbation with a purpose of invoking a temporary polarization on the particles, followed by a "motivation" AC signal to facilitate transport of the polarized drug through the membrane [5,6]. With that in mind, two successive AC electric fields were created between counter Electrode 1 and interdigitated Electrodes 2 and 3 "shortened" together ("Circuit 1"), and separated interdigitated Electrodes 2 and 3 ("Circuit 2"). In this delivery model the purpose of

Circuit 1 is to invoke polarization and electrokinetic transport on the drug particles by operating at polarization frequency determined from the Clausius–Mossotti polarization factor analysis. Circuit 2 operates in AC iontophoretic mode influencing the particles transdermal transport and reducing the skin resistance by electroporation mechanism [18]. A switchboard designed “in-house” transferred excitation signals between Circuits 1 and 2 with under millisecond time delay. In addition, 1200 s long control experiments were performed, both with the drugs present at the donor chamber without any external electrical excitations, and with Circuit 2 used to influence the drug delivery in a constant current (0.2 mA) iontophoretic mode, similar to currents used in commercially available iontophoretic devices. In the control experiments polarization of the drug particles utilizing Circuit 1 was not performed.

In order to verify the effectiveness of the drug delivery through the membranes, the pig skin and cow hoof samples were visually analyzed after each test for appearance of residue on the receiver chamber side, and for the changes in their electrical impedance [5–9]. The electrical impedance of the membranes was determined by the electric current and voltage drop across the samples according to Ohm's law. The studies also included temperature readings of the skin surface before, during and after each experimental study to determine the effects of electrical heating. Drug throughput into the receiver chamber was quantified using a UV–Vis concentration analysis technique in which study sample absorbencies were fit to a linear calibration curve of standard samples. The UV–Vis analysis (Varian Cary 300, Absorbance range 2–4 Abs; precision: ±0.002 Abs) at room temperature was performed and calibration curves of known drug concentrations (5 samples) were developed (terbinafine at 222 nm and insulin at 271.9 nm). After each

transdermal experiment, the receiver solution samples were collected. Three separate aliquots were taken from each solution; each of the three aliquots was scanned three times. The average of these nine values was used to fit the calibration curve for the peak UV absorbance measurements for the residue samples. The average standard deviation for the UV–Vis scans for Lamisil and Humalog® studies was 0.016 and the average relative error of the absorbance readings was 1.8%, with a range from 0.2% to 5.2%.

Lamisil has a number of surfactants that can potentially interfere with UV–Vis detection of terbinafine. Therefore, terbinafine transport was separately confirmed by GC-MS (Varian 3900/Saturn 2000), in which the components of a sample are separated and measured by their molecular mass and time of detection. The drug residue collected from the absorbent cloths was placed in methyline chloride or hexane solvents (each residue was dissolved in 10 mL solution and stored in30 mL amber bottles) before the GC-MS analysis. The intensity of the peaks could then be used to calculate the amount of terbinafine based on the standard samples.

*6.2.3 Experimental design and statistical analysis*

A series of studies was performed to investigate the transdermal transport and changes in the membranes' conductivities as a function of AC voltage amplitudes and frequencies, treatment time, and membrane thickness. This type of factorial design identifies the most important parameters affecting drug transport and pinpoints optimal ranges for those parameters. The resulting $5^3*2^2$ factorial design with two variables at two levels and five variables at three levels for insulin, and $4^3*2^2$ for terbinafine is summarized in table 13.

| Levels | Circuit 1 | | | Circuit 2 | | | Membrane Thickness mm |
|---|---|---|---|---|---|---|---|
| | Time (sec) | AC voltage amplitude (V) | Frequency (Hz) | Time (sec) | AC voltage amplitude (V) | Frequency (Hz) | |
| 1 | 100 | 0.1 | 1.0 | 100 | 0.1 | 0.1 | 1.0 |
| 2 | 1200 | 1.0 | 100 | 1200 | 1.0 | 1.0 | 1.5 |
| 3 | | 10 | 10000 | | 10 | 100 | 2.0 |

***Table 13**: Factorial design for terbinafine and insulin.*

This factorial design incorporates a total of 500 studies for insulin and 256 studies for terbinafine with the data analysis performed using StatGraphics OnlineR (StatPoint Technologies, Warrenton, VA) software. For each study two controls were incorporated, one without any electrical excitation; and one applying constant 0.2 mA current DC signal for 1200 s. A broader study of the effects of other input control parameters, such as geometry of the device; thickness, type and condition of the membrane; initial amounts and type of drugs; and localized external heating for regulating transdermal transport through animal and human skin model is being developed at that time.

## 6.3 Results and Discussion

### *6.3.1 Simulation of the AC electrokinetic forces*

Before conducting an experimental evaluation of the transdermal transport concept, a computational model was developed taking into consideration a variety of polarization and electrokinetic forces influencing drug particles in external non uniform AC electric field created by the asymmetrical Electrodes 2 and 3 and counter Electrode 1. The effects

of EP, EO, drag, and Brownian forces can be estimated from Smoluchowski, Helmholtz–Smoluchowski, Stokes, and Brown equations for small particles, respectively [24–27]. Joule heating temperature increase resulting from the application of external electric field can be estimated [25,26] for a fluid with conductivity σM and thermal conductivity k as $\Delta T=\sigma M E_{RMS}^2/k$, where ERMS is the root mean square value of the AC electric field [24]. An applied electric field and resulting localized Joule heating also result in temperature gradient in the medium and spatial variations in the conductivity, permittivity, viscosity, and density of the solution, creating inhomogeneous coulomb and dielectric body forces in a fluid. This phenomenon is known as the "electrothermal effect" and can induce microscale fluid motion, thereby non invasively stirring the fluid at the microscale. An order of magnitude estimation of the electrothermal flow was provided [25, 26] as $F_{ELTHERM}=E_{RMS}^2 (1/\varepsilon)(d\varepsilon/dT)/2$. The effect of the gravitational force was assumed to be negligible.

Manipulation of biological species by DEP is one of the most broadly applied microfluidic sorting methods. A dipole movement is induced on the biological particles when they enter non uniform AC field. Polarized particles incur AC frequency-dependent DEP force that is unique to the particle type and size. The time-averaged DEP force acting on a particle with radius a is estimated as $F_{DEP}= 2\pi a^3 \varepsilon_M \varepsilon_0 RE[K] grad E_{RMS}^2$. The real part of the Clausius–Mossotti factor $RE[K]=RE[(\varepsilon_P^* - \varepsilon_M^*)/(\varepsilon_P^* + 2\varepsilon_M^*)]$ represents the frequency-dependent mismatch in complex dielectric properties of the media ($\varepsilon_M^*$) and the particles ($\varepsilon_P^*$). Variations in this factor give rise to a DEP force that is frequency dependent and unique for a particle type. The DEP force can induce selective particle movement to regions of high or low potential field, depending on the

polarizability of the particles compared with that of the suspending media, and resulting positive or negative value of the Clausius–Mossotti factor. “Positive” DEP force directs the particles toward the high potential region of the electric field, while a “negative” DEP propels the particles in the direction of decreasing field strength. The DEP mobility of a particle scales directly with its surface area, so that to manipulate small particles larger electric field gradients are required [34]. Thus by using a mismatch in conductivity and permittivity values of medium and particles, submicron non polar particles can be elegantly manipulated on planar and 3D interdigitated electrodes in steady pool and continuous flow.

A simulation of the electric field distribution between asymmetrical electrodes was modeled using ANSYS Multiphysics (Canonsburg, PA), a finite element software package. A two-dimensional model was sufficient to describe the electric fields created by Electrodes 1, 2 and 3. The result of the simulation shows that the electric field distribution is the strongest and the electric field gradient is at its maximum in the vicinity of the interdigitated Electrodes 2 and 3; particles which undergo positive DEP should be attracted to those regions. These estimates were conducted for particles located 10 μm from the plane of Electrodes 2 and 3. Figure 50 shows the frequency dependence of the Clausius–Mossotti polarization factor for insulin and terbinafine. It can be seen that both insulin and terbinafine experience positive DEP force at frequencies under 1 MHz, allowing to polarize and attract both drugs toward the region of higher field strength at the edges and in the gap between Electrodes 2 and 3.

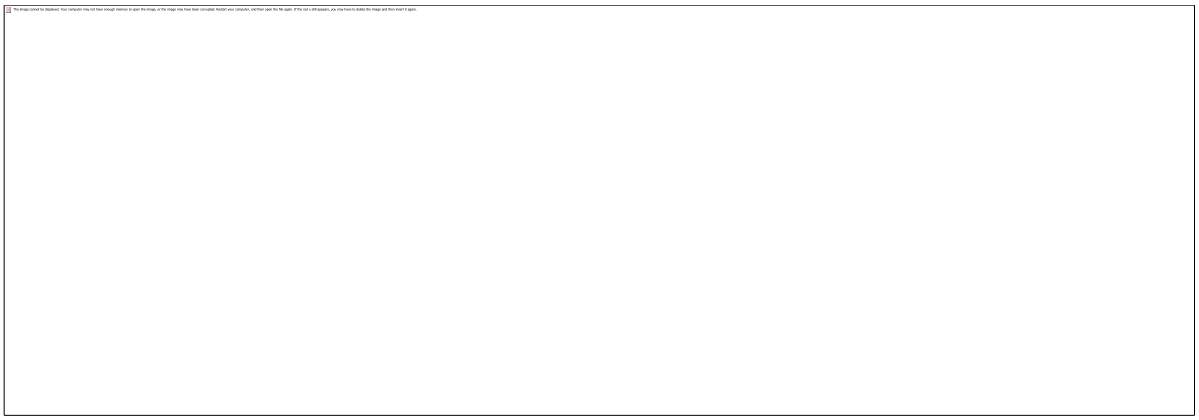

***Figure 50:*** *AC frequency dependence for Clausius–Mossotti polarization factor for: insulin (■) and terbinafine (▲).*

In agreement with the literature data for nanometer sized particles and ~μm-sized characteristic dimensions of irregular shaped electrodes [24–26], the estimated DEP force is predominant for insulin particles, in particular at higher applied electric fields (Figure 51A), resulting in total insulin velocity (when all other forces are taken into consideration) in 0.001–0.1 cm/s range for 1 to 10 V peak-to-baseline AC voltage amplitude range (Fig. 4). The effects of other forces, in particular those of Brownian, drag, electrothermal, and EO forces, are estimated to be negligible at AC voltages exceeding 0.2 V. Effects of Joule electrical heating are estimated to be minimal, reaching only ~0.01 °C at 10 V amplitude (Figure 52). Depending on the distance from the electrode surface and the applied electric field, the combined electrokinetic forces can transport insulin at millimeter-range distances in ~100 s. However, this effect of the DEP electrokinetics is only an estimate fully applicable to the particles located ~10 μm from the plane of Electrodes 2 and 3, as the predominant DEP force has a relative short-range effect. For the particles located further in the bulk solution, the EP force, and the concentration driven diffusion, are expected to attract the insulin particles closer to the plane of Electrodes 2 and 3.

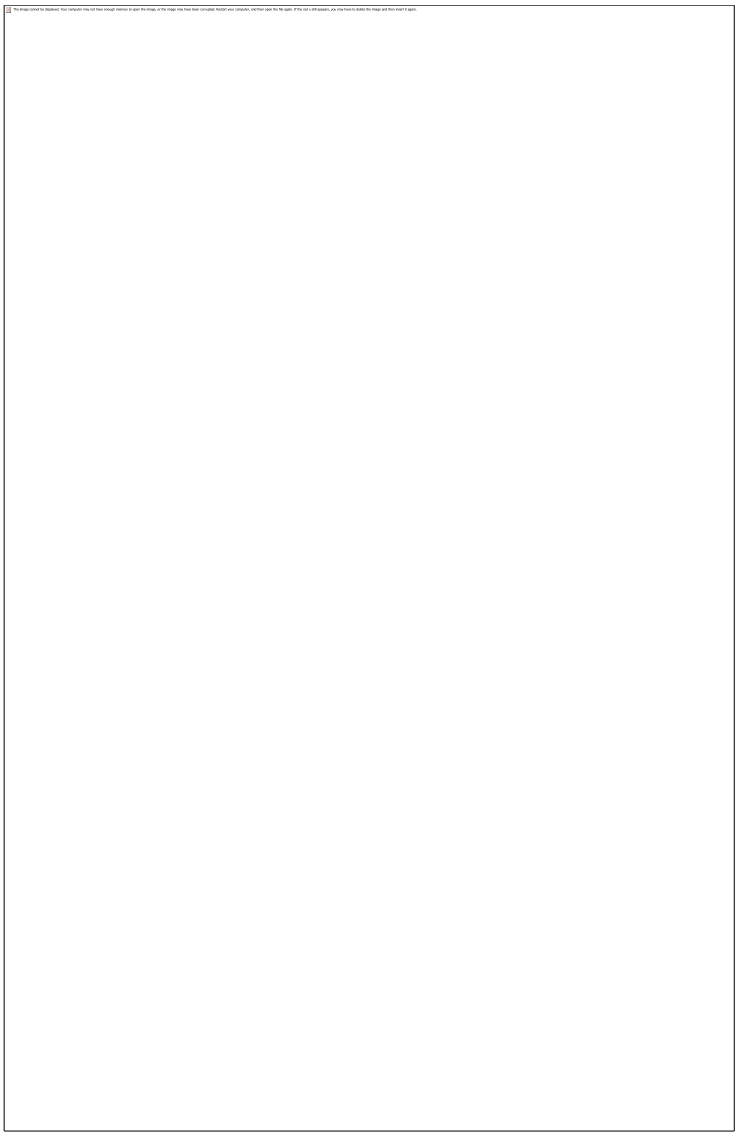

***Figure 51:*** *Simulated balance of DEP (■), EP (X), EO (▲), electrothermal (●), Brownian (◇), and drag (□) forces as a function of AC amplitude for: A) insulin; B) terbinafine.*

In the case of smaller and less polar terbinafine molecules, the DEP force is predominant above 1 V (Figure 51B). At lower fields the drag and Brownian forces become important. At higher electric fields the terbinafine particles total velocity is influenced by a combination of EP and DEP forces achieving total particles velocity in 0.0001–0.01 cm/s range for 1 to 10 V peak-to-baseline AC voltage amplitude range

(Figure 52). Effects of Joule electrical heating were estimated to be minimal, reaching ~0.002 °C at 10 V amplitude (Figure 51).

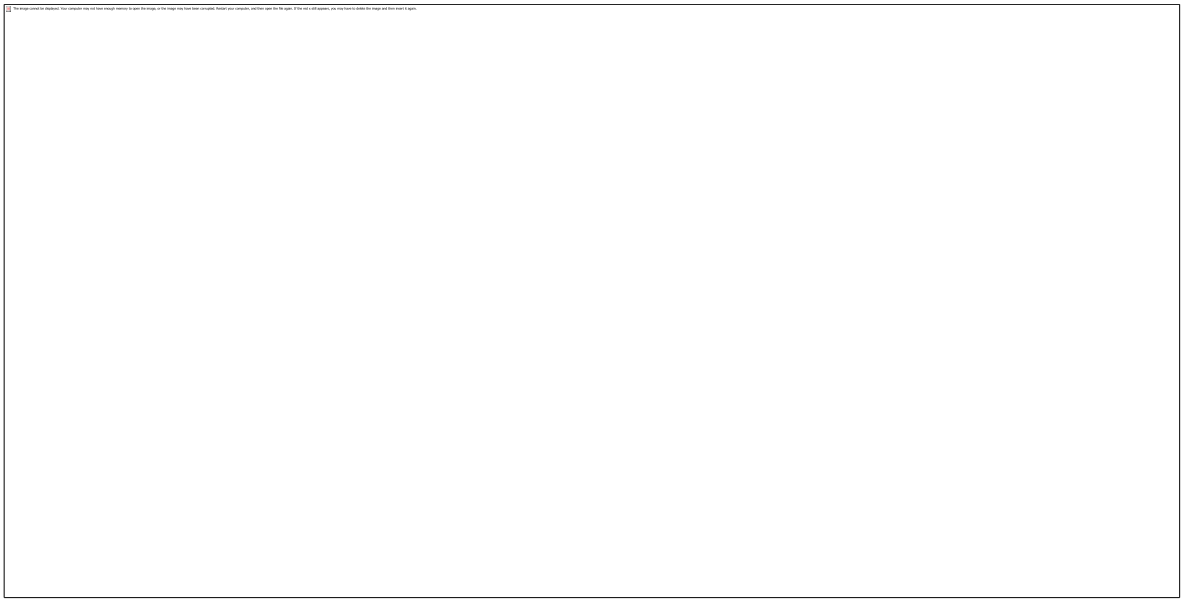

***Figure 52:*** *Estimated temperature increase for insulin (□) and terbinafine (●) and total velocities for insulin (■) and terbinafine (▲) as a function of AC voltage amplitude.*

*6.3.2 Insulin and terbinafine delivery results*

Statistical analysis of the results transmembrane transport demonstrated a 5–9 times increase in the pig skin conductivity for insulin delivery (the mean increase was 6.78±1.45 times) and a 2–5 times increase in the cow hoof conductivity for terbinafine delivery (the mean increase was 3.48±1.25 times) depending on the applied voltage amplitudes and frequencies, delivery time, and the membrane's thickness. The literature data suggests that AC and DC iontophoretic skin treatments produce reversible increases in hydration and disorganization in the lipid bilayers of the stratum corneum, resulting in up to three orders of magnitude decrease in the skin electrical resistance and expanded skin porosity, leading to higher efficiency of transdermal transport [5–9]. The significant conductivity increase was therefore taken as an initial indicator of a more facile drug

penetration through the membranes. The statistical analysis demonstrated that this conductivity change was driven mostly by the AC voltage amplitude and frequency of the applied signal in Circuit 2, and the AC voltage amplitude in Circuit 1 (table 14). The membrane's conductivity increase is higher for the lowest (0.1 Hz) frequency value and the highest voltage amplitude (10 V) in Circuit 2, in agreement with previously reported AC iontophoretic results [17, 18]. Delivery time (in either Circuits 1 or 2) was not found to be a significant factor, indicating the conductivity change was driven by the effect of the applied electric fields on the membranes, not by the mass transport mechanism. Apart from the effects of the AC voltage amplitude that induces polarization and electrokinetic transport on the particles, the signal parameters in Circuit 1 appear to be relatively unimportant in affecting the membranes' conductivity change. Pre- and post-test pig skin and cow hoof conductivity measurements for the control experiments (which applied the drug without the electrical signal) showed less than 10% change.

| Input factors | | Conductivity, Cow hoof | Conductivity, Pig skin | Throughput, Terbinafine | Throughput, Insulin |
|---|---|---|---|---|---|
| Circuit 1 | Time | -0.09 | +0.11 | +0.15 | +0.04 |
| | AC voltage Amplitude | +0.37 | +0.56 | +0.45 | +0.69 |
| | Frequency | -0.12 | -0.06 | +0.10 | +0.09 |
| Circuit 2 | Time | -0.12 | +0.09 | +0.05 | +0.02 |
| | AC voltage Amplitude | +0.57 | +0.66 | +0.35 | +0.34 |
| | Frequency | -0.32 | -0.49 | -0.45 | -0.62 |
| Membrane Thickness | | N/A | -0.25 | N/A | -0.68 |

***Table 14:*** *R-values for input factors dependence in changes of cow hoof and pig skin conductivities and Terbinafine and insulin delivery throughput.*

A factor analysis of the investigating variables and one outcome measure (membranes' conductivity) finds three significant factors — Circuit 1 voltage, Circuit 2 voltage, and Circuit 2 frequency variables. The Circuit 1 voltage variable factor explains 28% (insulin) and 22% (terbinafine) of the variance in the outcome measures, Circuit 2 voltage factor explains 32% (insulin) and 42% (terbinafine), and Circuit 2 frequency explains 22% (insulin) and 24% (terbinafine), for a total of 82% (insulin) and 88% (terbinafine) of variance explained by the three factors. This indicates that although the study has captured most of the major influential factors, other variables, such as membrane thickness that was investigated only in Humalog®

experiments and showed a moderate (r= −0.25) negative effect on membrane conductivity change, also contribute to variations in outcomes.

The actual trans-membrane drug delivery was quantified by spectrophotometry and GC-MS. A certain degree of uncertainty is expected from the UV–Vis analysis of the solutions collected from the receptor compartment, as it detects only the portion of the drug passed completely through the entire membrane; an additional portion of the drug may be embedded in the membrane. Following the Lamisil transport tests, a residue optically comparable to terbinafine was discovered at a receiver chamber side of the membranes. GC-MS analysis confirmed the presence of terbinafine with essentially no interference from the other Lamisil cream components in this residue.

Quantification of the terbinafine transport using the developed drug delivery model demonstrated the drug delivery to the receiver side of the cow hoof membrane in 25%–53% range with a statistical mean of 39% based on an initial dose of 1% terbinafine. Transport by weight ranged from 1.25 μg to 2.65 μg. When only Electrodes 2 and 3 were used in the iontophoresis mode at a constant current of 0.2 mA for 1200 s, the UV–Vis analysis demonstrated 5.3% transport efficiency, similar to what was reported before in the literature on iontophoretic delivery. The passive application of the drug resulted in no detectable transport through the cow hoof membrane in 1200 s.

Quantification of insulin transport through the pig skin membrane demonstrated a throughput ranging from 12% to 97%, with a statistical mean of 57% based on an initial insulin amount of 2.85 mg in 500 μL sample. Membrane thickness has shown strong negative correlation ($r = -0.68$) with throughput, indicating that thicker membranes are more effective in impeding the insulin transport. When only Electrodes 2 and 3 were used in the iontophoresis mode at a constant current of 0.2 mA for 1200 s, the UV–Vis analysis demonstrated at most 2% transport efficiency (within the error of the UV-

analysis), indicating essentially no measurable insulin transport. The passive application of insulin resulted in no transmembrane transport improvement in 1200 s. Circuit 2 parameters affecting the transdermal transport were AC voltage and frequency, with higher voltage amplitude and lower frequency providing a significant nearly linear transport enhancement (Figure 53A), similarly to the previously published data [18].

For both experimental sets with Lamisil and Humalog® it was shown that the AC frequency values for the electric signals applied in Circuit 1 played essentially no role in the effectiveness of the drugs transport. This is not surprising considering that Clausius–Mossotti polarization factor values for both drugs are positive and constant at frequencies under 100 kHz, therefore including all three AC frequency values used in Circuit 1 (1, 100, and 10,000 Hz) (Figure 50). In compliance with the initial premise that the electrokinetic forces increase either proportionally to the electric field or proportionally to the gradient of the square of the electric field, increasing the AC voltage amplitude in Circuit 1 resulted in an increase in throughput from 7±2% (0.1 V) to 40±13% for terbinafine transport (10 V) in 1200 s. Increasing of the AC amplitude from 0.1 V to 10 V (Humalog®) resulted in the increase in throughput from 10±2% to 74±20% for insulin transport in 1200 s. Figure 53 illustrates this point by presenting the data samples for the experiments where the thickness of the membranes was held constant at 1 mm, operational times for both Circuits 1 and 2 at 1200 s, Circuit 1 AC frequency at 1000 Hz, Circuit 2 AC frequency at 0.1 Hz, and Circuit 2 voltage peak-to-baseline amplitudes variable between 1 and 10 V. Delivery times for Circuit 1 played little role in the effectiveness of the drugs delivery, showing weak positive correlation (r=0.04 for insulin, r=0.15 for terbinafine) with throughput, indicating that longer delivery times are

somewhat more effective in increasing drug transport. Relative weakness this correlation may be related to one of the computational analysis conclusions indicating that a time period of ~100 s is largely sufficient for polarization and transport of both drugs (in particular insulin) to the edges of Electrodes 2 and 3.

Apart from the effects of the voltage amplitudes in Circuits 1 and 2, and low frequency values in Circuit 2 for both investigated drugs, and membrane thickness in Humalog® studies, the investigating variables did not strongly correlate with throughput, which was fairly consistent across study parameters. For example, for the insulin studies half of the throughput values were between 40% and 70%, and three quarters were between 40% and 100%. The standard deviation for throughput was 22%.

Application of higher AC electric fields can potentially cause a heating Joule effect, especially if the media possesses abnormally high electrical and low thermal conductivities. The temperature readings of the skin surface before, during and after each experimental study demonstrated essentially no localized heating or visible damage to membranes (such as burns) due to the application of the electrical fields, consistent with the conclusions derived on the basis of the computational model (Figure 52).

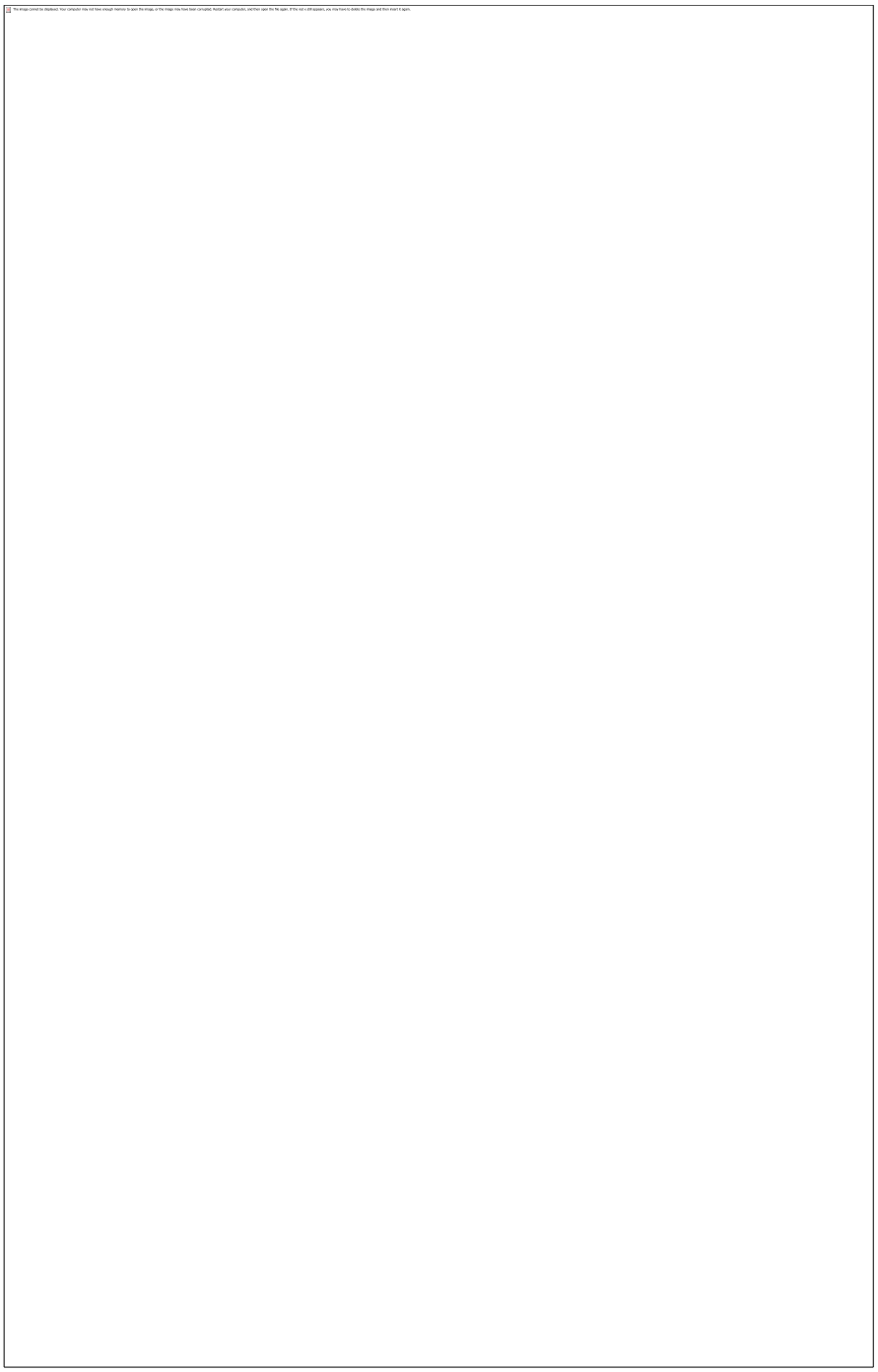

***Figure 53****: Drug delivery throughput results and variation by AC voltage amplitude in Circuit 1 for: A) insulin and B) terbinafine for the membranes thickness of 1 mm, Circuit 1 and Circuit 2 delivery times 1200 s, Circuit 1 AC frequency of 1000 Hz and Circuit 2 AC frequency of 0.1 Hzwere constant, Circuit 2 voltageamplitudes (■,■)10 Vand1 V(▲,▲). Iontophoresis results at 0.2 mA constant current (♦, ♦) are shown for comparison.*

Even for 10 V peak-to-baseline voltage amplitude in Circuit 2, the resulting AC currents did not exceed 5 mA (peak-to-baseline), which is a threshold based on human tolerance to these currents from the in vivo studies [19]. A comparable study in the literature showed that a low voltage current at 1 V for 1 min across the stratum corneum (10 μm thick and resistance 100 k Ohm/cm) gave rise to a very moderate 0.14 °C temperature increase [5]. However, this model assumes that all electrical energy is dissipated and converted into heat in the skin and generally provides an overestimate in the temperature rise. On the other hand, in the iontophoretic delivery a precaution should always be taken to keep the voltage amplitudes reasonably low while keeping the transdermal flux high. Due to the heterogeneity of the stratum corneum structure and composition, current could flow through localized pathways and dissipation of the energy could result in localized heating underestimated by calculation.

Development of microfabricated 3D interdigitated electrodes allows for a higher throughput drug delivery system as the EP and DEP effects are enhanced. These types of interdigitated devices show less of a decrease in the force profile with the distance above the plane, therefore greatly improving the polarization effect and transport of the particles. The interdigitated 3D electrodes structure also showed approximately 10 times smaller Joule heating effect for similar conditions when compared with a 2D planar electrodes structure [27].

Our results indicate that utilization of electric field in iontophoretic or electroporation skin treatment, even when strong enhancement in the skin conductivity is achieved, is insufficient for an effective transdermal delivery. The significant increase in the membrane conductivity is not always indicative of the efficient drug transport through

the membrane. In fact, the several studies with highest membranes conductivity increase (up to 10 times) had relatively low throughput values, including the lowest value recorded of 12% insulin throughput. The pathway of ion transportation induced by AC electrokinetic forces may be somewhat different from that induced by DC iontophoresis [17]. Non-facilitated transport across the skin can conceivably occur via transcellular, paracellular, or appendageal paths [28]. Transport pathways are influenced by physicochemical factors (molecular size, electric charge, concentration) and biological factors (skin site, morphological structure, regional blood flow). Although our study does not reveal the nature of the major transportation pathway during the AC electrokinetic delivery of terbinafine and insulin, their molecules may be transported through not only an appendageal path, but also a transcellular path. Additionally, we cannot deny the possibility that an AC electric field with a certain frequency may directly open a new pathway, leading to facilitation of ion transportation. Since structural changes in the biological membranes during the application of AC electrokinetic treatment were not examined in the present study, further research is needed to determine the major transportation pathway evoked by the AC field in different biological membranes. The effects of different biological membranes, including the human skin, will be addressed in the future, including the effects of membrane's heterogeneity and ageing.

### 6.4 Conclusions

Our results indicated that a combination of two applied AC fields generating electrokinetic and iontophoretic protocols was capable of in vitro transporting clinically significant amounts (50–90% throughput levels) of macromolecular insulin and non polar

terbinafine across membranes up to 2 mm thick in as little as several minutes, which is a significant improvement over macromolecular transdermal delivery results reported in the literature. On average, a combination of electrokinetic and iontophoretic protocols achieved transdermal delivery enhancement of ~28 times for insulin and ~7 times for terbinafine comparing to the iontophoretic constant current mode, and even better enhancement over the passive diffusion transdermal drugs application. This adaptable new method of drug transport was capable of motivating chemical compounds that are difficult to transport non invasively because of their large molecular size and non ionic structure. This is accomplished through the use of electrokinetic forces in interdigitated electrodes applying a non uniform AC electric field to a chemical compound, inducing an electrical field gradient that provides an electromotive force variable in magnitude and direction with applied frequency and field strength. Macromolecular drugs are thus polarized, and their iontophoretic transmembrane delivery is controlled by a second AC field. Applied AC voltage amplitude which polarizes the drugs, AC voltage amplitude and frequency inducing iontophoretic and electroporation effects, and the membrane's thickness were the most significant factors in affecting the throughput.

It is important to state that stand alone constant current iontophoretic mode application unsupported by electrokinetic polarization and manipulation of the drugs was generally unsuccessful in transdermal transport of insulin and terbinafine. Therefore the iontophoretic and electroporation enhancements of transmembrane delivery should be combined with electrokinetic polarization of non polar macromolecular drugs. The full magnitude of effects of the electrodes geometry and polarity; delivery time; medication chemical properties and composition; type, hydration, porosity, surface charge and

condition of biological tissue membranes; AC voltage amplitude and frequency on the efficiency of the electrokinetic drug transport is yet to be investigated. Continuing our work in optimization of combination (either sequential or simultaneous operation) of optimally- tuned AC electrical fields is needed for inducing polarization and enhancing transport to deliver macromolecules through biological membranes. On the basis of these principles, a non-invasive transdermal method capable of delivering non polar high molecular weight drugs appears to be feasible. This method has a potential for producing clinical products for efficient, facile, controlled and safe transdermal drug delivery.

## References


1. R. Langer, Transdermal drug delivery: past progress, current status, and future prospects, Adv. Drug Delivery Rev. 56 (2004) 557–558.
2. J. Varshosaz, Insulin delivery systems for controlling diabetes, recent patents on endocrine, Metab. Immune Drug Discovery 1 (2007) 25–40.
3. P. Batheja, R. Thakur, B.B. Michniak, Transdermal iontophoresis, Expert Opin. Drug Delivery 1 (2006) 127–138.
4. N. Dixit, V. Bali, S. Baboota, A. Ahuja, J. Ali, Iontophoresis — an approach for controlled drug delivery, Curr. Drug Delivery 4 (2007) 1–10.
5. V. Preat, R. Vanbever, Skin electroporation for transdermal and topical drug delivery, in: R. Guy, J. Hadgraft (Eds.), Transdermal Drug Delivery, Drugs and the Pharmaceutical Sciences, 123, Marcel Dekker, 2003, pp. 227–254.
6. A. Jadoul, J. Bouwstra, V. Preat, Effects of iontophoresis and electroporation on the strateum corneum. Review of the biophysical studies, Adv. Drug Delivery Rev. 35 (1999) 89–105.
7. A. Jadoul, J. Doucet, D. Durand, V. Preat, Modifications induced on stratum corneum structure after in vitro iontophoresis; ATR-FTIR and X-ray scattering studies, J. Controlled Release 42 (1996) 165–173.
8. S. Thysman, D. Van Neste, V. Préat, Noninvasive investigation of human skin after in vivo iontophoresis, Skin Pharmacol. 8 (5) (1995) 229–236.
9. P.J. Canatella, M.R. Prausnitz, Prediction and optimization of gene transfection and drug delivery by electroporation, Gene Ther. 8 (2001) 1464–1469.

10. Y.W. Chien, O. Siddiqui, Y. Sun, W.M. Shi, J.C. Liu, Transdermal iontophoretic delivery of therapeutic peptides/proteins. I: insulin, Ann. N.Y. Acad. Sci. 507 (1987) 32–51.
11. A.K. Banga, Y.W. Chien, Hydrogel based iontotherapeutic delivery devices for transdermal delivery of peptide/protein drugs, Pharm. Res. 10 (1993) 697–702.
12. S.K. Gupta, K.J. Bernstein, H. Noorduin, A. Van Peer, G. Sathyan, R. Haak, Fentanyl delivery from an electrotransport system: delivery is a function of total current, not duration of current, J. Clin. Pharmacol. 38 (1998) 951–958.
13. A. Kim, P.G. Green, G. Rao, R.H. Guy, Convective solvent flow across the skin during iontophoresis, Pharm. Res. 10 (1993) 1315–1320.
14. M.J. Pikal, The role of electroosmotic flow in transdermal iontophoresis, Adv. Drug Delivery Rev. 46 (2001) 281–305.
15. W.I. Higuchi, S.K. Li, A.-H. Ghanem, H. Zhu, Y. Song, Mechanistic aspects of iontophoresis in human epidermal membrane, J. Controlled Release 62 (1999) 13–23.
16. S.K. Li, A.-H. Ghanem, K.D. Peck, W.I. Higuchi, Pore induction in human epidermal membrane during low to moderate voltage iontophoresis: a study using AC iontophoresis, J. Pharm. Sci. 88 (1999) 419–427.
17. H. Inada, A.H. Ghanem, W.I. Higuchi, Studies on the effects of applied voltage and duration of human epidermal membrane alteration/recovery and the resultant effects upon iontophoresis, Pharm. Res. 11 (1994) 687–697.

18. G. Yan, K.D. Peck, H. Zhu, W.I. Higuchi, S.K. Li, Effects of electrophoresis and electroosmosis during alternating current iontophoresis across human epidermal membrane, J. Pharm. Sci. 94 (2005) 547–558.
19. S.K. Li, W.I. Higuchi, H. Zhu, S.E. Kern, D.J. Miller, M.S. Hastings, In vitro and in vivo comparisons of constant resistance AC iontophoresis and DC iontophoresis, J. Controlled Release 91 (2003) 327–343.
20. G. Yan, S.K. Li, W.I. Higuchi, Evaluation of constant current alternating current iontophoresis for transdermal drug delivery, J. Controlled Release 110 (2005) 141–150.
21. S.K. Li, W.I. Higuchi, H. Zhu, Y. Song, Methods for delivering agents using alternating current, US Patent 6512950 (2003).
22. A. Marcus, Diabetes care — insulin delivery in a changing world, Clin. Rev. Medscape J. Med. 10 (5) (2008) 120.
23. S. Devasenathipathy, J.G. Santiago, Electrokinetic flow diagnostics, in: K. Brewer (Ed.), Micro- and Nano-Scale Diagnostic Techniques, Springer, New York, 2003, pp. 1–19.
24. P.K. Wong, T.-H. Wang, J.H. Deval, C.-M. Ho, Electrokinetics in micro devices for biotechnology applications, IEEE/ASME Trans. Mechatron. 9 (2) (2004) 366–376.
25. H. Ramos, N. Morgan, N. Green, A. Castellanos, AC electrokinesis: a review of forces in microelectrode structure, J. Phys. D: Appl. Phys. 31 (1998) 2338–2353.

26. H. Morgan, A. Izquierdo, D. Bakewell, N. Green, A. Ramos, The dielctrophoretic and traveling wave forces generated by interdigitated electrode arrays: analytical solution using Fourier series, J. Phys. D: Appl. Phys. 34 (2001) 1553–1561.
27. F. Tay, L. Yu, A.J. Pang, C. Iliescu, Electrical and thermal characterization of a dielectroiphoretic chip with 3D electrodes for cells manipulation, Electrochim. Acta 52 (2007) 2862–2868.
28. T. Kinoshita, T. Shibaji, M. Umino, Transdermal delivery of lidocaine in vitro by alternating current, J. Med. Dent. Sci. 50 (2003) 71–77.
29. N. Sugai, Recent developments in pharmacology and clinical use of pentazocine, Masui 40 (1991) 1037–1041.
30. B.A. Berkowitz, J.H. Asling, S.M. Shnider, Relationship of pentazocine plasma levels to pharmacological activity in man, Clin. Pharmacol. Ther. 10 (1969) 320–328.
31. G.C. Giakos, Aqueous insulin and alcohol macromolecules and multiphasic molecular systems with enhanced photophysical signal characteristics and multifunctional properties, Int. J. Signal Imaging Syst. Eng. 1 (1) (2008) 41–50.
32. D.C. Carrer, C. Vermehre, L.A. Bagatolli, Pig skin structure and transdermal delivery of liposomes: a two photon microscopy study, J. Controlled Release 132 (2008) 12–20.
33. D. Mertin, B.C. Lippold, Bovine hoof — in-vitro permeability of the human nail and of a keratin membrane from bovine hooves: prediction of the penetration rate of antimycotics through the nail plate and their efficacy, J. Pharm. Pharmacol. 49 (9) (1997).

34. M.W. Wang, Using dielectrophoresis to trap nanobead/stem cell compounds in continuous flow, J. Electrochem. Soc. 156 (8) (2009) G97–G102.